

**CENTRAL RESPIRATORY CIRCUITS THAT CONTROL DIAPHRAGM
FUNCTION IN CAT REVEALED BY TRANSNEURONAL TRACING**

by

James H. Lois

B. S. in Neuroscience, University of Pittsburgh, 2006

Submitted to the Graduate Faculty of
Arts and Sciences in partial fulfillment
of the requirements for the degree of
M. S. in Neuroscience

University of Pittsburgh

2008

UNIVERSITY OF PITTSBURGH

ARTS AND SCIENCES

This thesis was presented

by

James H. Lois

It was defended on

July 30, 2008

and approved by

J. Patrick Card, PhD

Linda Rinaman, PhD

Alan Sved, PhD

Thesis Advisor: J. Patrick Card, PhD

Copyright © by James H. Lois

2008

CENTRAL RESPIRATORY CIRCUITS THAT CONTROL DIAPHRAGM FUNCTION IN CAT REVEALED BY TRANSNEURONAL TRACING

James H. Lois, M. S.

University of Pittsburgh, 2008

Previous transneuronal tracing studies in the rat and ferret have identified regions throughout the spinal cord, medulla, and pons that are synaptically linked to the diaphragm muscle; however, the extended circuits that innervate the diaphragm of the cat have not been well defined. The N2C strain of rabies virus has been shown to be an effective transneuronal retrograde tracer of the polysynaptic circuits innervating a single muscle. Rabies was injected throughout the left costal region of the diaphragm in the cat to identify brain regions throughout the neuraxis that influence diaphragm function. Infected neurons were localized throughout the cervical and thoracic spinal cord with a concentration of labeling in the vicinity of the phrenic nucleus where diaphragm motoneurons are known to reside. Infection was also found throughout the medulla and pons particularly around the regions of the dorsal and ventral respiratory groups and the medial and lateral reticular formations but also in several other areas including the caudal raphe nuclei, parabrachial nuclear complex, vestibular nuclei, ventral paratrigeminal area, lateral reticular nucleus, and retrotrapezoid nucleus. Infection was also localized in fastigial and dentate deep cerebellar nuclei. Additionally infected neurons were observed in the midbrain, particularly in the periaqueductal grey matter and mesencephalic reticular nucleus but also in other regions including the pedunclopontine nucleus, cuneiform nucleus, Edinger-Westphal nucleus, nucleus

locus coeruleus, and the red nucleus. Diencephalic labeling was most concentrated within the regions of the perifornical area and the medial parvocellular division of the paraventricular nucleus of the hypothalamus but was also found in several other areas. Infected neurons were also observed in the cruciate sulcus of the cerebral cortex as well as in prefrontal and insular cortices. This data suggests that the central circuits innervating the diaphragm muscle in the cat are highly complex and integrated with the central circuits controlling a variety of other non-respiratory behaviors.

TABLE OF CONTENTS

PREFACE	xii
I. INTRODUCTION	1
II. METHODS	9
A. ANIMALS	9
B. VIRUS	9
C. SURGICAL PROCEDURES	10
D. TISSUE PREPARATION	11
E. IMMUNOHISTOCHEMISTRY	12
F. ANALYSIS	13
III. RESULTS	15
A. INTRODUCTION	15
B. METHODOLOGICAL CONSIDERATIONS	16
C. SPINAL CORD INFECTION	18
D. MEDULLARY RESPIRATORY GROUPS	21
E. MEDIAL RETICULAR FORMATION	24
F. LATERAL RETICULAR FORMATION	25
G. VENTRAL PARATRIGEMINAL NUCLEUS	26
H. LATERAL RETICULAR NUCLEUS	26
I. RAPHE NUCLEI	27

J.	VESTIBULAR NUCLEI	27
K.	RETROTRAPEZOID NUCLEUS	29
L.	CEREBELLUM	29
M.	PARABRACHIAL NUCLEAR COMPLEX	30
N.	OTHER MEDULLARY AND PONTINE NUCLEI	31
O.	MIDBRAIN LABELING	32
P.	DIENCEPHALON	36
Q.	CORTEX	38
IV.	DISCUSSION	39
A.	INTRODUCTION	39
B.	SPECIFICITY OF VIRUS TRANSPORT	40
C.	SPINAL CORD INFECTION	41
D.	INFECTION OF THE MEDULLARY RESPIRATORY GROUPS	42
E.	RETROTRAPEZOID NUCLEUS AND CHEMORECEPTION	45
F.	APNEA	46
G.	POSTURAL ADJUSTMENT AND RESPIRATION	48
H.	VOMITING	49
I.	LOCOMOTION AND RESPIRATION	51
J.	RESPIRATION AND SLEEP	52
K.	RESPIRATORY COMPONENTS OF STRESS	53
L.	VOLUNTARY CONTROL OF RESPIRATION	56
M.	INFECTION IN VISUAL AND AUDITORY PATHWAYS	57
N.	INFECTION IN DORSAL COLUMN NUCLEI	57

V. CONCLUDING REMARKS	59
APPENDIX A: LIST OF ABBREVIATIONS	60
APPENDIX B: TABLES AND FIGURES	61
BIBLIOGRAPHY	78

LIST OF TABLES

Table 1: Total numbers of infected neurons counted bilaterally within infected areas of the medulla, pons and cerebellum. The check marks (✓) indicate the presence of infection as determined by qualitative analysis. Abbreviations are indicated in the list of abbreviations.... 61

Table 2: Total number of infected neurons counted bilaterally within infected areas of the midbrain, diencephalon and cortex. Check marks (✓) indicate the presence of infection as determined by qualitative analysis. Abbreviations are indicated in the list of abbreviations.... 63

LIST OF FIGURES

Figure 1: Photomicrographs of infected neurons in the C5 spinal cord of animal C21. A: photomontage of the entire C5 spinal gray matter of one section. Boxes denote regions depicted at higher magnification in subsequent panels. The left side of the section is ipsilateral to the rabies injections into the diaphragm. B: a dense cluster of presumed motoneurons in the ventral horn. C: A group of infected presumed interneurons in Rexed's lamina X and the medial portion of lamina VII. D: A group of infected presumed interneurons concentrated in Rexed's lamina V. E: Infected presumed interneurons in medial lamina VII and lamina VIII contralateral to the side of injections. Bars designate 500 μm in panel A and 250 μm in the other panels..... 64

Figure 2: Locations of presumed interneurons labeled following the injection of rabies virus into the diaphragm. A and B: locations of labeled cervical interneurons in an early infection (animal C21, panel A) and an intermediate infection (animal C51, panel B) case. Representative transverse sections from each cervical segment are shown; the level is indicated on the section. C: locations of labeled interneurons in horizontal sections through the T5-T9 thoracic spinal cord of intermediate infection case C38. The gray matter is indicated as a shaded area, and the rostral end of the sections is towards the left side. The top section is through the intermediate zone, the portions of Rexed's lamina VII and X near the level of the central canal (CC). The bottom section is through the ventral horn. No sections that were clearly through the dorsal horn contained any infected neurons, and thus are not provided..... 65

Figure 3: A: Histograms illustrating the average number of infected presumed interneurons per section in each cervical spinal cord segment. The C8 segment was not processed for case C52. Error bars indicate one standard deviation. B: The average cell count per section from panel A expressed relative to the maximal value obtained for any cervical segment in a particular animal (i.e., the segment with the maximal average number of interneurons per section is indicated as having a 100% relative infection). C: The average percentage of infected presumed interneurons per section that was located in the ventral horn (Rexed's laminae VII-X) in each cervical spinal cord segment. Error bars indicate one standard deviation..... 66

Figure 4: Photomicrograph at 40X magnification of a medial reticular formation neuron in the *intermediate* animal C51 that illustrates the distribution of viral antigen within infected neurons. Note the homogeneous distribution of immunoreactivity within the cytoplasm as well as the punctate staining typically observed on the soma and dendrites of a rabies infected neuron.... 67

Figure 5: Maps of sections from an *early* (C52) and an *intermediate* (C39) case illustrating the localization of rabies infected neurons within the medulla 12.1 mm posterior to the interaural plane. Each dot in the maps represents a single labeled neuron. The dorsal respiratory group and

the rostral ventral respiratory group are within the boxes in each map. Photomicrographs illustrate the morphology and distribution of labeled cells in these regions from an *early* (C52) and an *intermediate* (C51) case. The photomicrographs connected to boxes in the maps by two lines were taken from the same section used to create the map. Photomicrographs connected to boxes by a single line with an arrowhead are from an analogous case. All photomicrographs were taken at 10X magnification and the scale bars in each photomicrograph represent 200 μm 68

Figure 6: Maps of sections through the dorsal and ventral respiratory columns in two *early* (C52 and C21) cases and one *intermediate* (C39) case. Each dot represents a single infected neuron. The dorsal (DRG) and ventral (VRG) respiratory columns are depicted with the ovals drawn on each map. A-C illustrate the caudal VRG at 16 mm posterior from the interaural plane, D-F illustrate the DRG and the rostral VRG at 12.1 mm posterior from the interaural plane, G-I illustrate the DRG and pre-botzinger complex at 11.6 mm posterior from the interaural plane, and J-L illustrate the Botzinger complex at 10 mm posterior from the interaural plane..... 69

Figure 7: Maps and photomicrographs illustrating the distribution and morphology of infected neurons in the regions of pre-Bötzing and Bötzing complex. Photomicrographs were taken at 10X magnification from the same sections used to create the corresponding maps. Pre-Bötzing maps and photomicrographs are from a section located 11.6 mm posterior to the interaural plane, and Bötzing maps and photos are from a section located 10 mm posterior to the interaural plane. Scale bars in both photomicrographs represent 200 μm . Each dot on the maps represents a single infected neuron..... 70

Figure 8: Maps of sections from two *early* (C52 and C21) and an *intermediate* (C39) case displaying the distribution of infected neurons in the rostral medulla and pons. A-C are located at 8.5 mm posterior to the interaural plane and D-F are located at 3.1 mm posterior to the interaural plane. Each dot represents a single labeled neuron. Photomicrograph in A illustrates an infected lateral vestibular nucleus neuron, the photomicrograph in B displays the labeled neurons in the medial reticular formation, the photomicrographs in C present infected neurons in the fastigial and lateral vestibular nuclei. The Kölliker-Fuse nucleus is illustrated in the photomicrographs in D and F. All photomicrographs were taken at 10X and scale bars represent μm 71

Figure 9: Maps and photomicrographs from an *early* (C21) and an *intermediate* (C39) case depicting the distribution and morphology of infected neurons in the ventral paratrigenial nucleus. Photomicrographs are from the same sections used to create maps. Both photomicrographs were taken at 10X magnification and both scale bars represent 200 μm 72

Figure 10: The top histogram displays the number of infected neurons at nine different levels throughout the medial reticular formation in each animal. The bottom panel displays the percentage of infected neurons at each level of the medial reticular formation relative to the number of neurons at the maximally infected level. The distance of each level posterior to the interaural plane is indicated in mm..... 73

Figure 11: A: Total number of infected neurons in the Kölliker-Fuse nucleus counted on the ipsilateral and contralateral sides of the brain in each animal. B: The total number of infected neurons counted in the medial parabrachial nucleus on ipsilateral and contralateral sides of the brain in each animal. C: The total number of infected neurons counted on the ipsilateral and contralateral sides of the lateral parabrachial nucleus in each animal. D: Total number of infected neurons in the red nucleus on the ipsilateral and contralateral sides of the brain in each animal with red nucleus infection..... 74

Figure 12: Maps of sections through the midbrain from two *intermediate* animals at different stages of infection (C38 and C51). A-B are located at 0.6 mm posterior to the interaural plane, C-D are located at 1.6 mm anterior to the interaural plane, and E-F are located 5.2 mm anterior to the interaural plane. The photomicrograph in B illustrates the morphology of infected neurons in the mesencephalic reticular nucleus, the photomicrographs in C and D depict the morphology of infected neurons in the lateral periaqueductal gray matter, and the photomicrograph in F depicts the morphology of infected neurons in the red nucleus. Photomicrographs connected to the corresponding boxed brain area in a map with two lines are taken from the same section used to create the map. Photomicrographs connected to the boxed brain areas with a single line are from an analogous section in a different animal. Each dot in the maps represents a single infected neuron and each photomicrograph was taken at 10X magnification. All scale bars represent 200 μm 75

Figure 13: Maps of sections through the diencephalon from an *intermediate* case (C51). The section mapped in A is located at 11 mm anterior to the interaural plane, the map in B is from a section located 11.8 mm anterior to the interaural plane, and the section mapped in C is 12 mm anterior to the interaural plane. The photomicrograph in B was taken at 10X magnification from the same section used to create the corresponding map and illustrates the morphology of infected neurons in the parvocellular division of the paraventricular nucleus of the hypothalamus. The photomicrograph in C was taken at 5X magnification and depicts the morphology of labeled neurons in the perifornical area from a *late* case (C36). Apparent differences in the laterality of infection in maps of sections is due to the angle at which the tissue was cut. Infected neurons were distributed bilaterally in labeled areas within these maps..... 76

Figure 14: Photomicrographs of the cruciate sulcus from a *late* (C36) and an *intermediate* (C39) animal. Both photomicrographs were taken in the portion of the cruciate sulcus depicted in the schematic situated between the photos. The photomicrograph in A was taken at 10X and it illustrates the morphology of infected neurons in the cruciate sulcus from a *late* case. The photomicrograph in B was taken at 20X and depicts the morphology of a single neuron in the cruciate sulcus from an *intermediate* case..... 77

PREFACE

Acknowledgments go to my sponsor Bill Yates and my committee members J. Patrick Card, Linda Rinaman, and Alan Sved for their support and guidance throughout the duration of this project. Thanks also go to Cory Rice and Bill Yates for their participation in gathering data and analyzing infection in the spinal cord.

INTRODUCTION

Respiration, an essential function, is controlled by the central nervous system (CNS). The inspiratory and expiratory phases of respiration are controlled by the action of several muscles, but during normal or quiet breathing contraction and relaxation of the diaphragm muscle alone is sufficient to cause respiration. During heavy breathing, additional muscles are needed to force air into and out of the lungs. These muscles include inspiratory muscles like the external intercostals and expiratory muscles like the abdominal muscles and internal intercostals (Miller et al., 1997). In order to perform the rhythmic act of breathing, the neural inputs of these muscles must be coordinated in the CNS. Additionally respiration is modulated during several behaviors like exercise or postural adjustment (Yates et al., 2002). These observations suggest that the central control of respiration is an integrated process that is controlled by multiple cell groups throughout the neuraxis (Ezure, 1996; Lindsey et al., 1994).

Two columns of neurons in the medulla have been implicated as the major players in the generation and integration of respiratory signals that are sent to motoneuron pools controlling the muscles of respiration in the spinal cord. These columns include the dorsal respiratory group (DRG), which is concentrated in the ventrolateral nucleus of the solitary tract, and the ventral respiratory group (VRG), which is found in the ventrolateral medulla in close association with the nucleus ambiguus and retrofacial nucleus (Cohen, 1981; Connelly et al., 1992). These cell groups have been well characterized by a number of physiological studies in the cat that functionally defined them based on their firing patterns in relation to respiration (Cohen, 1979).

The DRG was defined as a functionally homogenous group of inspiratory neurons, but the ventral respiratory group was divided into several functional subdivisions based on the differential location of inspiratory and expiratory neurons along its rostrocaudal axis. The first division of the VRG was made at the level of the obex from which expiratory neurons were found to extend about 3 mm caudally and inspiratory neurons were found in a column extending about 3 mm rostrally (Haber et al., 1957). These expiratory and inspiratory groups of neurons were called caudal and rostral VRG respectively. Later electrophysiological studies discovered the existence of another expiratory center, termed the Bötzing complex, found just rostral to the rostral VRG at the level of the retrofacial nucleus (Lipski and Merrill, 1980; Merrill, 1981). Even more recently, the transitional zone between rostral VRG and Bötzing has been classified as a separate region called the pre-Bötzing complex that contains a mixture of inspiratory and expiratory neurons as well as phase spanning neurons that fire during the transition between inspiration and expiration. This subdivision was first delineated on the basis of its pacemaker properties observed in neonatal rats (Smith et al., 1991), but has since been considered a separate functional subdivision in cats as well (Connelly et al., 1992).

In order to further characterize how the DRG and VRG influence respiration efforts were made to identify the projections of these groups. Extensive antidromic stimulation and spike triggered averaging studies were done in cats to reveal the projections of DRG and VRG inspiratory and expiratory neurons within the medulla and to the spinal cord (Berger, 1977; Davies et al., 1985; Ezure, 1990; Fedorko et al., 1983; Fedorko and Merrill, 1984; Hoskin and Duffin, 1987a; Hoskin and Duffin, 1987b; Merrill and Lipski, 1987; Merrill et al., 1983). Additionally, these projections were characterized by anterograde tracing studies using horseradish peroxidase injected intracellularly into identified inspiratory or expiratory neurons

(Otake et al., 1989; 1990; Otake et al., 1987; Sasaki et al., 1989). These studies revealed that the DRG and VRG are highly integrated groups consisting of excitatory and inhibitory connections among themselves and to respiratory motoneurons in the spinal cord. However, to get a better understanding of the entire population of projections within these groups and to the spinal cord, tracing studies were performed involving the injection of the anterograde tracers, tritiated amino acid or phaseolus vulgaris leucoagglutinin (PHA-L), into the DRG and VRG (Cohen, 1981; Loewy and Burton, 1978; Otake et al., 1988). These studies revealed dense projections between the DRG and subdivisions of the VRG as well as to interneurons in the spinal cord and motoneurons controlling the muscles of respiration, making a substantial contribution to the literature concerning the neural control of respiration.

Anterograde tracing experiments revealed the population of projections from the DRG and VRG, but the results of these experiments became more reliable when retrograde tracing studies from targets of the DRG and VRG produced similar findings. Such retrograde tracing studies involved the injection of horseradish peroxidase into the phrenic nuclei of rats and cats (Onai and Miura, 1986; Onai et al., 1987; Rikard-Bell et al., 1984). The phrenic nuclei, located in the ventral horn of the fourth, fifth, and sixth cervical segments of the spinal cord, house the motoneurons that innervate the diaphragm. These studies revealed the pattern and morphology of neurons in the DRG and VRG that influence functioning of the diaphragm. Morphological analysis in the cat revealed mostly medium or small multipolar and fusiform cells throughout the DRG and VRG. These findings were consistent with anterograde tracing studies that revealed projections to the phrenic nuclei from the DRG and VRG. Additional retrograde tracing studies were performed involving the injection of horseradish peroxidase into the DRG and VRG populations of the cat (Kalia et al., 1979; Smith et al., 1989). Dense projections were found from

a number of medullary and pontine sites including the parabrachial nuclear complex, medial reticular formation, raphe nuclei, and retrotrapezoid nucleus. Subsequent stimulation and lesion studies have implicated these regions in specific functions that are coordinated with respiratory muscle activity. The parabrachial complex has been implicated in producing a variety of respiratory modulations including apneusis (Alheid et al., 2004), the medial reticular formation is thought to be involved in producing emesis (Miller et al., 1996), and the raphe and retrotrapezoid nuclei have been implicated in modulating respiration in response to chemosensory signals (Nattie, 2001).

As a whole the electrophysiological and monosynaptic anterograde and retrograde tracing literature has revealed a great deal about the circuitry influencing function of the respiratory muscles. The DRG and rostral VRG have been identified as the main source of excitatory projections to diaphragm motoneurons and the caudal VRG has been identified as the source of excitatory projections to motoneurons of the muscles of expiration (abdominals and internal intercostals). The Bötzing complex was also found to project to diaphragm motoneurons, but in this case the projections were inhibitory, consistent with this group's role in expiration. The Bötzing complex also makes inhibitory connections with the DRG, rostral VRG, and caudal VRG giving this area the capability of inhibiting inspiration as well as expiration. These projection patterns provide the Bötzing complex the ability to modulate respiration in a variety of ways to produce specific patterned behaviors like emesis. Indeed the Bötzing complex has been shown to be active during emesis and is likely responsible for the inhibition of the inspiratory DRG and rostral VRG centers during the act of vomiting (Miller et al., 1997). The DRG and rostral VRG also project to each other as well as to the caudal VRG, but the main source of connections within the DRG and VRG respiratory groups comes from the pre-

Bötzinger complex. Most projections from pre-Bötzinger are within the respiratory groups with just a few projections going to the spinal cord. This group sends inhibitory projections to expiratory neurons in the Bötzinger complex and caudal VRG as well as inhibitory projections to inspiratory neurons in the DRG and rostral VRG. Additionally pre-Bötzinger has excitatory connections to the inspiratory neurons of the DRG and rostral VRG (Ezure, 1996). The large number of connections that pre-Bötzinger has with the entire extent of the dorsal and ventral respiratory groups give this area the capability of controlling the activity of the entire DRG and VRG populations, an observation that is consistent with the idea that this area is involved in rhythmogenesis (Smith et al., 1991).

The development of viral transneuronal tracing technology has provided the most recent advancement in our understanding of the synaptology of central respiratory circuitry. Studies employing pseudorabies virus (PRV) for retrograde tracing from phrenic nuclei or directly from the diaphragm in rats and ferrets have been particularly influential (Billig et al., 2000; Dobbins and Feldman, 1994; Yates et al., 1999). The time-dependent transynaptic movement of this viral tracer allowed identification of higher order circuitry that influences diaphragm function leading to considerations about the neural circuitry that coordinates respiratory muscle activity with other behaviors. Furthermore, interspecies differences in these findings implicated particular brain sites in coordinating respiration with other behaviors. For example, injections of PRV into the diaphragm of ferrets produced a much greater quantity of labeled neurons in the medial reticular formation than was found in similar retrograde tracing experiments involving rats. Ferrets, unlike rats, are capable of emesis, and thus the infected medial reticular formation neurons in the ferret could be involved in coordinating respiration with emesis. But despite the illumination that these recent tracing studies have offered in identifying the neuronal circuitry

that influences diaphragm function, they only focused their findings on medullary and pontine areas. Thus the identification and organization of the neural circuitry within areas of the midbrain, diencephalon, and cerebral cortex that influence diaphragm function were not well characterized. An additional transneuronal tracing study conducted in the mouse did examine labeling in higher centers. This study involved injections of rabies virus into both the diaphragm and intercostal muscles (Gaytán et al., 2002). They found retrogradely labeled cells throughout the DRG and VRG as well as in other brainstem sites including the medial reticular formation, parabrachial nuclear complex, Barrington's nucleus, nucleus subcoeruleus, locus coeruleus, and the lateral superior olive. Within the cerebellum labeled neurons were concentrated in the fastigial nucleus, and in the midbrain labeling was mostly found throughout the periaqueductal gray and pedunculopontine nuclei with a few scattered cells labeled in the deep mesencephalic nucleus and superior colliculus. The hypothalamus also contained a few labeled cells in the lateral and anterior hypothalamic nuclei as well as in zona incerta. Additionally a few cells were labeled in the laterodorsal, dorsomedial, and posterior thalamic nuclei. In the cortex several labeled neurons were found in the frontal and parietal cortices. The findings of this study include brain areas that likely influence respiration by modulating it in accordance with other behaviors. However, since this study involved transneuronal tracing from both diaphragm and intercostal muscles it is hard to make specific functional correlations with their findings. A more elegant approach to identifying how higher brain centers influence respiratory activity could involve injecting a transneuronal retrograde tracer into a single respiratory muscle. This type of experiment would yield more specific results concerning what aspects of respiration are modified by higher brain centers. The diaphragm muscle would likely be the best candidate for such a

study because the greatest understanding of central regulation of respiratory muscle activity is in relation to the diaphragm.

Diaphragm activity is coordinated with a variety of non-respiratory behaviors, which involve brain regions throughout the CNS. For example, diaphragm activity has been shown to correlate with locomotion in the cat (Iscoe, 1981; Kawahara et al., 1989), a behavior that involves the mesencephalic locomotor region in the midbrain (Jordan et al., 2008). In fact, previous studies have identified neurons in the mesencephalic locomotor region as well as in the caudal hypothalamus that when stimulated produce simultaneous increases in locomotion and respiration (Horn and Waldrop, 1998). Also, changes in posture alter diaphragm activity via the influence of the vestibular nuclei, fastigial nuclei, and medial reticular formation (Yates et al., 2002). Additionally alterations in respiration and thereby diaphragm activity are associated with transitions between sleep and wakefulness, and several midbrain and diencephalon areas have been identified that contribute to the control of sleep/wakefulness (Saper et al., 2005). In fact, one study identified retrogradely labeled neurons in the hypocretin population, located in the perifornical area of the hypothalamus, following injection of the retrograde tracer Cholera Toxin B into the phrenic nuclei of rats (Young et al., 2005). This study, however, failed to investigate retrograde tracing into brain regions other than the hypocretin population. Vocalization is also associated with modulation of diaphragm activity (Miller et al., 1997), and has been shown to be mediated through the periaqueductal gray matter in the midbrain (Holstege, 1989; Zhang et al., 1994). The midbrain periaqueductal gray matter is also involved in producing emotional responses to stress in cats that are accompanied by modulation of cardiorespiratory parameters (Bandler et al., 2000). The cerebral cortex is also likely to contain neuronal populations that project to areas that innervate the diaphragm. Recording, stimulation, lesion, and functional

imaging studies have implicated the cerebral cortex in contributing to voluntary modulation of breathing (Horn and Waldrop, 1998; Miller et al., 1997). There is considerable evidence that brain centers throughout the CNS are involved in modulating diaphragm activity in association with a variety of complex behaviors, but the organization of the neural circuits that synaptically link these brain centers with innervation of the diaphragm muscle have not been well described.

This study aimed to identify the extended neural pathways that contribute to diaphragm function with a particular emphasis on the midbrain, diencephalon, and cortex via transneuronal retrograde tracing with the N2C strain of rabies virus in the cat. The cat was chosen for this study largely based on the extensive body of respiratory electrophysiological literature that exists for this animal but also because cats are capable of complex behaviors that are associated with activity of the diaphragm muscle, like emesis. Previous transneuronal tracing studies of diaphragm circuitry were performed in rats and ferrets, but ferrets lack the electrophysiological literature on respiration and rats are not capable of emesis. Most previous transneuronal tracing studies looking at diaphragm circuitry employed pseudorabies virus (PRV) as the tracer, however, PRV is not an effective retrograde transneuronal tracer in cats (Card et al., 1997). Thus rabies virus was chosen as the tracer for this experiment. This virus has been shown to be successful in the retrograde transneuronal tracing of neural circuitry in a variety of species (Kelly and Strick, 2000). By injecting the virus into the diaphragm and analyzing the temporal progression of labeling throughout the central nervous system the location and hierarchy of brain regions that influence diaphragm function were established. The hypothesis underlying this study was that several brain areas throughout the CNS would be retrogradely labeled following injection of rabies into the diaphragm and that these areas would include sites that have been functionally implicated in behaviors that are coordinated with respiration by previous studies.

METHODS

ANIMALS

Fourteen 6-12 month old female cats (Liberty Research Inc.; Waverly, NY) weighing 2.6 to 3.5 kg were used in these experiments. The animals were not vaccinated for rabies and additionally their blood was examined for the presence of antibodies against rabies antigens to ensure that they did not have immunity to the virus. The animals were housed individually and maintained under a 12:12 hour light/dark cycle at 72°F. Prior to the onset of experiments animals were moved to a facility approved for BSL2 experiments. The animals were acclimated to the BSL2 laboratory for a minimum of 2 days before being injected with rabies virus and lived in the facility through the post inoculation interval. All procedures were approved by the Institutional Animal Care and Use Committee at the University of Pittsburgh and conformed to the Centers for Disease Control and National Institutes of Health requirements for the use of infectious pathogens (*Biosafety in Microbiological and Biomedical Laboratories*, 5th edn. U.S. Government Printing House, Washington, DC, 2007).

VIRUS

Several recent studies have utilized rabies virus as a transneuronal tracer of multisynaptic pathways (Kelly and Strick, 2000; Moschovakis et al., 2004; Rathelot and Strick, 2006; Ugolini, 1995). These studies demonstrated that rabies virus is transported exclusively in the retrograde direction with no evidence of being taken up by fibers of passage. It is well documented in these

studies that rabies does not cause cell lysis and is transported in a time-dependent manner, allowing identification of a hierarchy of multisynaptic circuits innervating specific targets.

The N2C strain of rabies virus was utilized for injections into all 14 animals. The transport properties of this strain of rabies virus have been well characterized (Kelly and Strick 2000). Dr. Peter Strick of the University of Pittsburgh provided the stocks of virus at a titer of 1×10^8 plaque forming units per ml. The virus was stored at -80°C and thawed just before injection. Excess virus was inactivated with Clorox and disposed of as biohazardous waste in accordance with the regulations imposed by the University of Pittsburgh Department of Environmental Health and Safety.

SURGICAL PROCEDURES

Surgical procedures were conducted under aseptic conditions within a rabies dedicated surgical suit approved for BSL 2 activities. Animals were initially anesthetized using ketamine (15 mg/kg) and acepromazine (1 mg/kg) injected i.m., and subsequently intubated and maintained under deep anesthesia with 1-2% isoflurane vaporized in O_2 . After shaving and scrubbing the animal's abdomen with betadine, the ventral surface of the diaphragm was approached via a midline incision through the skin and musculature of the abdominal wall. The viscera were retracted to expose the diaphragm and injections of rabies virus, diluted 1:300 in sterile water, were made under the peritoneal lining with a 25 μl Hamilton syringe equipped with a 22-gauge needle. Injections of 25 μl in volume were made at eight to twelve sites throughout the left costal region of the diaphragm to deliver a total of 200-300 μl of virus. At each site the inoculum was injected approximately 5-10 μl at a time in several second intervals as the needle remained in the diaphragm. Additionally the needle was kept in the diaphragm for several

seconds after completion of each injection to minimize leakage of the virus. Upon completion of the inoculations the peritoneal surface of the diaphragm was swabbed with cotton to absorb any leaked virus, and the abdominal musculature and skin were sutured shut. Heart rate and breathing rate were continuously monitored throughout surgery and body temperature was maintained with a heating pad. After animals had recovered from surgery they were returned to the BSL-2 rabies-dedicated isolation suite. For analgesia, animals received ketoprofen (injected i.m.) every 24 hours for 3 days (2 mg/kg initial dose and 1mg/kg maintenance dose). The health and well being of the animals was monitored at a frequency of at least every 8 hours until they were anesthetized and perfused at the conclusion of the experiment.

TISSUE PREPARATION

After survival times ranging from 61.5 to 144 hours (Table 1) animals were anesthetized using ketamine (15 mg/kg) and acepromazine (1 mg/kg) injected i.m., followed by sodium pentobarbital (40 mg/kg) injected i.p. After verifying the absence of nociceptive reflexes the animals were transcardially perfused with approximately 1 liter of heparinized saline followed by approximately 2 liters of 4% paraformaldehyde-lysine-periodate fixative (PLP) (McLean and Nakane, 1974). The brains and spinal cords were then removed and postfixed 1-2 days in PLP at 4°C, and cryoprotected in 30% sucrose in 0.1M phosphate-buffered saline (PBS) for two days. Spinal cord and brain sections were cut with a freezing microtome at a thickness of 40 µm. Thoracic spinal cord was sectioned horizontally and sequentially collected in 4 wells of phosphate-tris-azide buffer (PTA). Cervical spinal cord was sectioned coronally and sequentially collected in 4 wells of PTA. The medulla, pons, midbrain, and diencephalon were also sectioned coronally but sequentially collected in 6 wells of PTA. Cortex was either cut

sagittally (n=12) or coronally (n=2) and collected in 6 wells of PTA. Tissue sections were stored at 4°C in PTA until being processed for immunohistochemical localization of rabies virus.

IMMUNOHISTOCHEMISTRY

Sections from at least one well of tissue from all areas of each animal were processed for immunohistochemical localization of rabies virus using avidin-biotin immunoperoxidase techniques (Hsu et al., 1981). Sections were incubated in 0.3% hydrogen peroxide in distilled water for 30 minutes to quench endogenous peroxidase activity. After several rinses in PTA or 0.1M (PBS) sections were incubated in 1.5% normal horse serum in PTA or 10 millimolar (mM) PBS for 20 minutes with agitation. After rinsing sections were incubated in a mouse monoclonal antibody directed against the rabies virus phosphoprotein (M957, diluted 1:300 in PTA) for 18-72 hours at 4°C. The specificity of this antibody to rabies virus has been established previously (Nadin-Davis et al., 2000). After being brought to room temperature sections were rinsed several times at 5 minute intervals in phosphate tris (PT) or PBS buffer and incubated in biotinylated secondary antibody (1:200, biotinylated horse antimouse IgG, Vector Laboratories) in 10mM PBS or PT for 30 minutes with agitation at room temperature. Sections were rinsed again and incubated in 1% ABC complex (Vector) in PT or 10mM PBS for 1 hour. The A and B Vectastain reagents were combined 30-60 minutes before being used. Sections were again rinsed in PT or PBS and then incubated in a saturated solution of filtered 3, 3'-diaminobenzidine in PT with 0.0002% hydrogen peroxide for 3 minutes or until the reaction was complete as determined by visual inspection. Sections were then rinsed in PT or PBS, mounted on gelatin-coated slides, cleared in ascending concentrations of ethanol followed by 3 changes of xylene, and

coverslipped with cytoal. Most sections were counterstained with neutral red for identification of cytoarchitecture.

ANALYSIS

Sections were initially examined qualitatively to determine the pattern of infection. The distribution of infected neurons in the brainstem, midbrain, and diencephalon of six cases was mapped using the Stereoinvestigator image analysis system (MicroBrightField, Inc.; Williston, VT) interfaced with a Nikon microscope at 40X magnification. Neuronal cell bodies were only counted if they contained a homologous distribution of antigen within their cytoplasm and the cell nucleus was visible.

Sections through the medulla, pons, cerebellum, and midbrain were mapped at a frequency of every fifth section from one well of tissue. Initial qualitative analysis demonstrated that this frequency provided an accurate representation of labeling within the most heavily infected cell groups. Comparable sections were mapped in all animals that were included in the quantitative analysis. Similarly, the quantitative mapping of labeled neurons in the diencephalon focused upon the areas that were identified as being heavily infected in initial qualitative analysis. Sections through the Fields of Forel, perifornical area, parvocellular division of the paraventricular nucleus of the hypothalamus, intralaminar nuclei of the thalamus, ventrolateral nucleus of the thalamus, and paraventricular nuclei of the thalamus were mapped in comparable sections using the image analysis system. The boundaries of specific areas were determined using the Berman cat atlas (Berman, 1968) and digital feline brain atlases (<http://BrainMaps.org>). Cortex sections were examined qualitatively.

Maps of cervical spinal cord sections were made for eight animals. In cases that had a small to moderate number of infected cells in the spinal cord, maps were made at a frequency of every 4th section. In cases with more advanced spinal cord infection 2 sections were mapped from each cervical spinal cord segment. The thoracic spinal cord of each animal was qualitatively examined to determine the relative quantity of labeled neurons at different levels. The locations of infected cells in the thoracic cord were noted with particular care taken towards identifying whether the intermediolateral cell column was infected. Selected sections were mapped in one case to demonstrate a lack of intermediolateral cell column infection.

Selected sections were photographed with a Zeiss Axioplan photomicroscope equipped with a Hamamatsu camera (Hamamatsu Photonics, Hamamatsu, Japan) and a Simple-32 PCI image analysis system (Compix, Lake Oswego, OR). Adobe Systems (San Jose, CA) Photoshop and Illustrator software were used for preparing photographs and maps of sections for publication. Brightness and contrast of images was adjusted without any other alterations.

RESULTS

INTRODUCTION

Injection of rabies virus into the diaphragm produced transneuronal labeling in the spinal cords and brains of 11 animals with survival times ranging from 61.5 to 144 hrs. There were 3 additional attempts at diaphragm injections that were unsuccessful in producing retrograde infection of CNS neurons after survival times ranging from 96 to 120 hours. The three animals with the latest survival times (120-144 hrs) had infections that were too advanced to define the route through which higher cell groups were infected. The eight animals used for analysis were categorized into *early*, *intermediate*, and *late* infection groups based on how extensive labeling was in these animals (Table 1). The *early* group was classified based on infection being confined to the spinal cord, medulla, and pons. The *intermediate* group involved cases with increased numbers of neurons in the areas labeled in *early* cases with the addition of newly labeled areas extending into the midbrain, diencephalon and cortex. The *late* group involved cases with heavier infection within areas that were labeled in *intermediate cases* with a few additional areas becoming labeled. The patterns of labeling within groups were consistent between animals, supporting the conclusion that rabies virus infected neurons through transneuronal passage of synaptically linked neurons. In the following sections we review the evidence for specific transneuronal transport of rabies virus in our material and then describe the temporal progression of viral transport through central circuits at various intervals following inoculation of the diaphragm. The circuitry is described from a regional perspective beginning

in the spinal cord and moving progressively higher in the neuraxis. The description of this circuitry includes a morphological analysis of infected cells and a quantitative comparison of labeling in the ipsilateral and contralateral sides of groups that were qualitatively determined to have marked differences in the laterality of infection.

METHODOLOGICAL CONSIDERATIONS

Rabies virus is a small (180 × 175 nm) enveloped RNA virus. Its genome codes for five proteins: nucleoprotein, phosphoprotein, matrix protein, glycoprotein, and polymerase. The exact mechanism of how rabies virus is transported has not been completely discerned but potential hypotheses with supporting evidence do exist. The rabies glycoprotein appears to be responsible for the entry of rabies virus into neurons as it binds to neuron-specific receptors such as the p75 neurotrophin receptor, neuron adhesion molecule (NCAM), or the nicotinic acetylcholine receptor (Finke and Conzelmann, 2005). Moreover it has been hypothesized that the axonal transport of rabies virus is accomplished by the binding of the rabies virus phosphoprotein to the dynein motor complex, which is responsible for shuttling molecules along microtubules towards the cell body.

The antiserum used in these experiments to identify infected neurons was raised against the phosphoprotein that resides in the infective nucleocapsid core of the rabies virus (Kelly and Strick, 2000). Thus, immunocytochemical localization of antigen provides a clear representation of viral replication, assembly and transport in infected neurons. Examination of the morphological distribution of viral antigen throughout the soma and dendrites of labeled neurons provided strong evidence for specific retrograde transneuronal transport of rabies virus through central circuits synaptically connected to phrenic motor neurons. At the earliest stages of

infection viral antigen was concentrated in the cell soma and proximal dendrites. Consistent with replication of an RNA virus that replicates in the cell cytoplasm, viral antigen was absent from the nucleus. Antigen within the soma and dendrites of labeled cells was homogeneously distributed and also accumulated within distinct puncta associated with the plasma membrane. At later stages of infection the distribution of viral antigen extended progressively into the dendrites of infected neurons and consisted of both homogenous staining and punctate accumulations of viral antigen similar to those observed on the cell soma. Light and electron microscopic analyses of pseudorabies virus have demonstrated that similar puncta reflect sites of transneuronal passage of virus (Card, 1995) and it is probable that this is also the case in our material. Figure 4 illustrates this punctate pattern of labeling in the soma and dendrites of a medial reticular formation neuron. The absence of cytopathology associated with infected neurons at all stages of infection was consistent with specific transneuronal passage of virus rather than nonspecific or lytic release into the extracellular space at all stages of infection. Additionally, viral antigen was not observed in glia, even in relation to neurons that had been replicating virus the longest. This observation is consistent with the conclusion that rabies virus specifically moved through neuronal pathways.

The consistent patterns of infection in populations of neurons throughout the brains of the animals used in this study provide additional evidence that rabies virus was being transported in a specific transynaptic manner. As the extent of infection increased in animals the same areas that were labeled in less advanced cases were labeled in more advanced cases. Similarly, as more areas became infected they were consistently infected in analogous cases. Additionally, the distribution of infected neurons respected boundaries of cell groups rather than expanding radially around infected neurons as one would expect if the virus was being released

indiscriminately. Also, the pattern of infection adhered to known connectivity, consistent with specific transynaptic transport. Figure 5 illustrates these points by showing maps and photomicrographs of infected neurons through the medulla of *early* and *intermediate* cases. The maps and photomicrographs reveal that as infection becomes more advanced the same areas that were labeled early are consistently labeled in later cases.

Despite the specific transneuronal transport that rabies virus was observed to have the progression of infection was not entirely defined on the basis of the postinoculation interval. Additional factors like the size of the animals also affected the progression of viral transport through specific circuits. Some animals that were larger had less advanced infections than animals that were smaller but had similar survival times. As such, the *early*, *intermediate*, and *late* groups that we used to classify the level of infection observed in animals was not directly correlated with their post-innoculation intervals.

SPINAL CORD INFECTION

In all animals deemed to have successful rabies inoculations into the diaphragm, large infected neurons were present in the central portion of the ventral horn of the C4-C6 spinal segments ipsilateral to the side injected with virus, between the medial and lateral columns of motoneurons. In all cases except animal C53, the large neurons formed a tight cluster, and so much reaction product was present that it was difficult to obtain an accurate count of the cells. An example of such a cell cluster in the C5 segment of animal C21 is shown in Figure 1A-B. The position of this cluster of large infected neurons in the gray matter corresponds to the known location of motoneurons innervating the diaphragm in the cat (Berger et al., 1984; Cameron et al., 1983; Rikard-Bell and Bystrzycka, 1980). As such, the cells were classified as putative

phrenic motoneurons. In animal C53, large infected neurons were present in a similar location, but the number was much lower than in the other cases (only 1-2 cells per section). Presumably, only a fraction of phrenic motoneurons was infected in this animal, likely because the post-inoculation survival time was >24 h shorter than in the other cases.

In addition to these large neurons, smaller infected cells were distributed bilaterally in the cervical spinal cord in every animal, and were deemed to be interneurons that were transneuronally infected by passage of rabies virus from phrenic motoneurons.

Photomicrographs of putative interneurons in the C5 segment of animal C21 are shown in panels C, D, and E of Figure 1. Figure 2A illustrates the locations of the putative interneurons in representative sections from each cervical segment of early infection case C21, whereas Figure 2B shows the locations of putative interneurons in intermediate infection case C51. The average number of infected presumed interneurons per section of each cervical spinal cord segment is shown in Figure 3A. This quantitative analysis considered every fourth section for animals with moderate numbers of infected spinal interneurons (cases C53, C21, C52, and C38). For animals with extensive infection in the spinal cord (C39, C51, C36, and C37), two sections per segment were considered for the analysis. The average values represent a pooling of cell counts from the left and right sides. Figure 3B shows the same average data as in 3A, but the values are expressed relative to those in the segment with the most extensive infection for a particular animal. All animals except C53, the case with the shortest survival time and fewest infected neurons, exhibited infected presumed interneurons in all cervical segments. In animal C53, however, the presumed interneurons were limited to the C2 and C5-C7 segments.

A consideration of Figure 3A-B reveals a correlation between the number of infected spinal cord neurons and how far rostrally the infection spread in the brain. In animals where

infection reached as far rostrally as the cortex (C36, C37, C39, C51), an average of > 300 labeled presumed interneurons were present per section in the most infected spinal cord segment. In animals where the infection reached no more rostrally than the pons (C21, C52, C53), an average of < 60 presumed interneurons were present per section in the most infected segment. In one animal (C38), virus was transported to the midbrain but no more rostrally; in this case, the spinal infection (average of 190 cells per section in the most infected segment) was intermediate between that in animals where infection reached the cortex and where it was confined to the medulla and pons. Furthermore, the distribution of presumed interneurons in the cervical spinal cord differed depending on the extent of infection in the brain. In the animals with the most advanced infections (C36 and C37), the relative number of labeled presumed interneurons was about the same in the upper cervical segments as in the C4-C7 segments. In contrast, in cases C21, C52, and C53, the amount of infection in C1-C2 was <15% of that in segments containing the diaphragm motoneurons. In animals C38, C51, and C39, the number of infected C1 neurons was 30-40% of that in C4-C6.

In all the sections shown in Figure 2A-B, the number of infected presumed interneurons in the dorsal horn (Rexed's laminae I-VI) is lower than in the ventral horn (laminae VII-X). The fraction of neurons in the ventral horn in each spinal cord segment is indicated in Figure 3C. Except for a few segments in the animals with the most extensive infections, the majority of labeling was confined to the ventral horn. In animals with early infection (C21, C52, C53), >70% of the presumed interneurons were located in the ventral horn in every segment. A number of other patterns were also observed with regards to the locations of the presumed interneurons. In all animals, an aggregation of labeled cells was present adjacent to the central canal, in medial lamina VII and lamina X of the segments containing diaphragm motoneurons

(see Figure 1C for an example). In animals with intermediate or advanced infection, infected neurons were present in the intermediolateral part of the gray matter and adjacent white matter of the upper cervical spinal segments, as indicated in Figure 2B. The locations of these cells correspond to those of a group of propriospinal interneurons identified through neurophysiological experiments as having inspiratory-related activity (Aoki et al., 1980; Nakazono and Aoki, 1994). However, this population of neurons was absent in animals with early infection, as indicated in Figure 2A.

Horizontal sections through the thoracic spinal cord were additionally examined for all animals. Infected neurons were observed in the upper thoracic cord in all cases, mainly in sections through the ventral horn and region near the central canal (intermediate zone). However, in animals C53, C21, C52, and C38, only a few scattered neurons were present caudal to the T4 segment. For example, Figure 2C shows the distribution of infected neurons in sections through the intermediate zone and ventral horn of case C38. In these four cases, no infected cells were observed along the lateral border of the gray matter, particularly in the intermediolateral region that contains sympathetic preganglionic neurons. However, the thoracic infection was much more extensive in the other cases, all of which also exhibited considerable infection in the brain that extended to the cortex. It is impossible to rule out the possibility that the intermediolateral cell column contained infected cells in these animals.

MEDULLARY RESPIRATORY GROUPS

Labeled cells were quantified throughout the dorsal and ventral subdivisions of the respiratory groups. Based on physiology studies, the dorsal respiratory group (DRG) is defined as a focal group of neurons concentrated in the ventrolateral nucleus of the solitary tract (vINTS)

0-2 mm rostral to the obex, 2.0-2.8 mm lateral to the midline, and 1.5-2.5 mm ventral to the medullary surface (Cohen, 1976). The obex is defined as the transitional zone where the central canal merges with the 4th ventricle. Our data agreed with this definition in that labeled neurons were concentrated in vINTS. However, while we found this group of neurons to be most concentrated in vINTS it was also seen to circumscribe the solitary tract to some extent and to extend as far as 3.1 mm rostral to the obex. The labeled neurons in the DRG were medium or small multipolar and fusiform cells distributed bilaterally. Fusiform cells were more concentrated in the region circumscribing the solitary tract dorsomedially from vINTS toward the medial nucleus of the solitary tract mNTS. At the earliest survival time (C53, 61.5 hrs) just 9 neurons were found in vINTS (Table 1). At the next *early* survival time (C52, 87 hrs) 152 neurons were present in vINTS and within the region surrounding the solitary tract dorsomedially from vINTS. At later survival times more labeled neurons were predominantly found in the region circumscribing the solitary tract. This can be seen in Figure 6, which illustrates the pattern of infection in the DRG of 3 animals with differing stages of infection. Figure 5 displays the morphology of neurons in the DRG with photomicrographs of the DRG in an *early* and *intermediate* animal.

The ventral respiratory group (VRG) has been defined as a continuous column of neurons in the ventrolateral brainstem (3-4 mm lateral to the midline and 3-5 mm ventral to the dorsal surface) that extends from the first cervical roots to the middle of the pons (Cohen, 1981). This column of respiratory neurons has been functionally subdivided based on the differential distribution of inspiratory and expiratory neurons. The caudal ventral respiratory group (cVRG) exists from the spinomedullary junction to the level of the obex in close proximity to the nucleus retroambiguus (Arita et al., 1987). The rostral ventral respiratory group (rVRG) is continuous

with the cVRG, extending 1.5 to 2.4 mm rostral to the obex in close proximity to the nucleus ambiguus. The Botzinger complex (BOT) lies between 3.1 and 4.7 mm rostral to the obex within the region of the retrofacial nucleus, and the pre-Botzinger complex (pre-BOT) exists at the transitional level between rVRG and BOT within the region of the compact division of nucleus ambiguus (Connelly et al., 1992). Our data revealed a continuous column of neurons in the ventrolateral medulla distributed bilaterally within the subdivisions described above. Infected neurons were mostly medium or small multipolar and fusiform neurons. Within the cVRG and rVRG, which provide dense projections to the spinal cord, labeled neurons were generally found to have larger soma than in the predominantly propriobulbar BOT and pre-BOT groups.

At the earliest survival time (C53) a few labeled neurons were found within all of the aforementioned divisions of VRG except for pre-BOT (Table 1). Most of the labeled neurons at this time (8 cells) were found in the rVRG. At the next *early* survival time (C52) more labeled neurons were found in each of the VRG subdivisions. Numbers of labeled neurons especially increased in rVRG (218 cells), BOT had slightly more infected neurons than pre-BOT (89 vs 79 cells), and with just 25 labeled neurons cVRG was the least labeled (Table 1). At later survival times numbers of infected neurons greatly increased in each subdivision with the most labeled neurons still found in the rVRG and the least number of labeled neurons found in cVRG. Table 1 reviews the number of labeled neurons in each subdivision of each animal. Figure 6 provides maps from 3 animals illustrating the pattern of infection in each subdivision of the VRG while Figure 5 and Figure 7 display photomicrographs illustrating the cell morphology in these areas.

MEDIAL RETICULAR FORMATION

Infected neurons in the medial reticular formation (MRF) were quantified throughout the medulla and pons, within the paramedian, magnocellular, and gigantocellular reticular fields illustrated in Berman's cat brain atlas (Berman, 1968). MRF infection was found in every animal except the one with the earliest survival time (C53). Labeled neurons in this region were mostly large multipolar cells that were distributed bilaterally. There was a differential distribution of labeled neurons within the caudal-rostral plane of this group. Figure 10 shows the number of infected MRF neurons in each animal through the caudal-rostral extent of the MRF from 13.5 to 4 mm posterior from the interaural plane. In each animal the greatest number of infected MRF neurons was found from 10 to 8.5 mm posterior to the interaural plane where neurons were most densely packed within the magnocellular reticular field located ventromedially in the MRF. In the paramedian and gigantocellular reticular fields labeled neurons were more diffusely scattered. There was not a clear morphological difference between labeled neurons in the different subfields of the MRF. There was a large increase in the number of labeled MRF neurons from animals in the *early* to the *intermediate* group (Table 1). In the *early* group the total number of MRF neurons counted ranged from 47 to 121 cells, while the *intermediate* group counts ranged from 538 to 1570 cells. Similarly there was a large increase in MRF infection from the animal with labeling confined to the midbrain (C38) to animals with infection in the diencephalon (C39 and 51). The animal that had infection reach the midbrain but no farther rostral had 538 infected neurons in MRF while animals with diencephalic labeling had 1491 to 1570 labeled neurons in MRF. Figure 6 and Figure 8 display MRF labeling with maps of sections from 3 animals at different stages of infection. Figure 8 also displays the morphology of infected cells in this region with a photomicrograph from an *early* case.

LATERAL RETICULAR FORMATION

The lateral reticular formation (LRF) was infected in all animals except for the one with the earliest survival time. Labeled neurons in this region were quantified throughout the medulla and pons within the lateral reticular field illustrated in Berman's cat brain atlas (Berman, 1968). Infection in the LRF was quantified from 18.3 to 3.1 mm posterior to the interaural plane. Counts of labeled neurons in VRG, which is found within the LRF, were not included in counts made in LRF. Infected cells in this region were mostly medium or small multipolar and fusiform cells that were distributed bilaterally. LRF infection was much greater in the medulla than in the pons in all animals. In the medulla the total number of infected neurons in LRF ranged from 84 to 919 cells while in the pons counts only ranged from 22 to 340 infected neurons. Additionally the number of labeled neurons increased greatly from *early* to *intermediate* survival groups (Table 1). In *early* groups total numbers of infected neurons throughout the LRF ranged from 106 to 336 cells but in *intermediate* groups counts ranged from 687 to 2055 infected neurons. Additionally, many more infected neurons were present in animals that had diencephalon labeling (C39 and C51) compared to the animal with labeling confined to the midbrain (C38). Only 687 infected neurons were observed in the LRF of the animal that had infection restricted to the midbrain while 1259 to 2055 labeled neurons were counted in animals with infection in the diencephalon. Figure 6 and Figure 8 illustrate the pattern of infection in this group with maps of sections from 3 animals at different stages of infection. It can be seen in Figure 6 that infected neurons in the medullary portion of LRF were located in the region surrounding the VRG and within the transitional area of LRF between the DRG and VRG. Moreover, since there was not a distinct morphological difference between cells in the VRG and the surrounding LRF, cell counts

in these regions may have been over or underestimated. There was always a clear density of neurons found in the ventrolateral medulla that could be classified as the VRG, however, at later survival times the boundary between this dense group and the surrounding LRF became difficult to discern.

VENTRAL PARATRIGEMINAL NUCLEUS

The ventral paratrigeminal nucleus (v5SP), defined as the area just ventral to the caudal spinal trigeminal nucleus in the muskrat (Panneton et al., 2000), was infected in all animals except the one with the earliest survival time (Table 1). Infected neurons in this region were mostly small fusiform cells with an occasional larger multipolar neuron present. Labeled neurons were found from 13.5 to 11.6 mm posterior to the interaural plane on both sides of the brain. In the *early* survival group numbers of neurons in v5SP ranged from 26 to 38 cells and in the *intermediate* survival group from 48 to 99 infected neurons were counted (Table 1). Figure 9 displays the pattern of infection and the morphology of infected neurons in v5SP with maps of sections and photomicrographs from an *early* and an *intermediate* animal.

LATERAL RETICULAR NUCLEUS

The lateral reticular nucleus (LRN), defined as a group of medium sized cells lining the ventrolateral caudal medulla from 16 to 10.8 mm posterior from the interaural plane (Berman, 1968), was infected in every case except for the one with the earliest survival time (C53). Infected neurons in this region were mostly medium sized multipolar cells that were distributed on both sides of the brain. In the *early* infection group numbers of labeled neurons in LRN ranged from only 1 to 9 labeled cells. At *intermediate* survival times 19 to 85 labeled cells were

found in LRN. A large jump in labeling of this region was observed between animals that had infection in the diencephalon and animals that did not. The animal with infection restricted to the midbrain (C38) had only 19 infected cells in LRN while the cases with diencephalic labeling (C39 and C51) had 75 to 85 labeled neurons in LRN (Table 1). Maps of sections through this region are illustrated in Figure 6 from 3 animals at different stages of infection.

RAPHE NUCLEI

The midline raphe pallidus (RP) and raphe obscurus (RO) nuclei have been defined in the cat by previous studies (Poitras and Parent, 1978). These caudal brainstem nuclei were infected in every animal except the one with the earliest survival time (C53). Infected neurons were observed in RO from 14.7 to 10 mm posterior from the interaural plane and in RP from 13.5 to 10 mm posterior from the interaural plane. A few infected cells were seen in *early* survival animals with just 1 to 2 neurons found in RP and 3 to 4 infected neurons found in RO. In the intermediate survival group several more labeled cells were found in these regions with 15 to 43 neurons found in RP and 4 to 31 infected neurons in RO. Just including animals with diencephalic infection (C39 and C51), 16 to 43 neurons were infected in RP and 20 to 31 labeled neurons were in RO (Table 1). Neurons in this region were mostly medium or small fusiform cells. Figure 6 and Figure 8 present maps of sections through these nuclei from 3 animals at different stages of infection.

VESTIBULAR NUCLEI

The vestibular nuclei consist of 4 separate anatomically distinct regions: the lateral vestibular nucleus (LVN), superior vestibular nucleus (SVN), inferior vestibular nucleus (IVN),

and the medial vestibular nucleus (MVN). The IVN is defined as a reticulated group of cells extending from 12.1 to 7.7 mm posterior from the interaural plane, 1.5 mm deep from the dorsal surface of the brainstem, and 3 mm lateral from the steep upslope of the wall of the 4th ventricle. The MVN is defined as a group of small packed cells extending from 10.8 to 6 mm posterior from the interaural plane, 1.5 mm deep from the dorsal surface of the brainstem, and 1.5 mm lateral to the steep upslope of the wall of the 4th ventricle. The LVN is defined as a group of large cells located 8.5 to 6 mm posterior from the interaural plane at the transitional zone between the brainstem and the deep cerebellar nuclei. Finally, the SVN is defined as a group of medium sized cells located from 6 to 5.2 mm posterior from the interaural plane, 1.5 mm deep from the dorsal surface of the brainstem, and 1.5 mm lateral from the steep upslope of the wall of the 4th ventricle (Berman, 1968).

None of these aforementioned vestibular nuclei were infected in the earliest survival animal (C53), and only the IVN and LVN were infected in the *early* survival group with 1 to 2 neurons found in IVN and 2 to 7 neurons found in LVN. In the *intermediate* survival group infected neurons were observed in all of the vestibular nuclei with 10 to 35 neurons found in MVN, 9 to 25 neurons found in SVN, 40 to 74 neurons found in IVN, and 31 to 257 neurons found in LVN. A large increase in infected LVN neurons corresponded with animals that had diencephalic labeling. In the *intermediate* survival animal that had infection restricted to the midbrain (C38) 31 infected neurons were observed and in animals that had labeling in the diencephalon (C39 and C51) 133 to 257 labeled neurons were counted (Table 1). Labeled cells in LVN were large and multipolar, cells in IVN and SVN were mostly medium sized and multipolar, and labeled neurons in MVN were small and round or fusiform. Infection was bilateral in each of these nuclei. Figure 8 illustrates the pattern of labeling in the LVN with maps

of sections in 3 animals at different stages of infection as well as the morphology of infected neurons in this region with photomicrographs from an *early* and an *intermediate* case.

RETROTRAPEZOID NUCLEUS

The retrotrapezoid nucleus (RTN) is defined as a dense group of cells located ventral to the retrofacial nucleus at its caudal end about 3.2 to 4 mm lateral to the midline. Rostrally this group is situated ventral and ventromedial to the facial nucleus and its rostral end lies at the level of the caudal pole of the superior olivary nucleus (Smith et al., 1989a). Only 1 labeled neuron was observed in the retrotrapezoid nucleus in a single *early* survival case (C21). In the *intermediate* survival group 16 to 29 infected neurons were observed bilaterally (Table 1). Infected neurons in this region were mostly small round or fusiform cells. There was not a large increase in labeling of this group in cases where the infection had reached the diencephalon. Figure 8 displays maps of sections that go through this group from 3 animals at different stages of infection.

CEREBELLUM

In most cases considered labeling in the cerebellum was confined to the deep cerebellar nuclei, which consist of the medially located fastigial nucleus that extends from 12.1 to 7.7 mm posterior from the interaural plane, the laterally located dentate nucleus that extends from 10 to 8.5 mm posterior from the interaural plane, and the interpositus nucleus that extends from 10 to 7.1 mm posterior from the interaural plane between the fastigial and dentate nuclei (Berman, 1968). Only a single neuron was observed in the fastigial and dentate cell groups from one *early* case (C21), but in *intermediate* animals numbers of labeled neurons ranged from 6 to 41 in the

fastigial nucleus and 1 to 24 in the dentate nucleus (Table 1). The *intermediate* animals that had infection in the diencephalon (C39 and C51) particularly showed a greater increase of infection in these nuclei compared to the *intermediate* animal with infection confined to the midbrain (C38). In C39 and C51 the fastigial nucleus contained 30 to 41 labeled neurons compared to the 6 infected neurons in C38, and the dentate nucleus contained 9 to 24 infected neurons compared to the 1 infected neuron found in C38. Labeled neurons in these nuclei were medium or small multipolar or fusiform cells. In the *late* survival group labeled neurons were also observed in nucleus interpositus and scattered throughout the purkinje cell layer of the cerebellar cortex. Figure 8 displays maps of sections through the fastigial and dentate nuclei from 3 animals at different stages of infection as well as a photomicrograph of infected neurons in the fastigial nucleus of an *intermediate* case.

PARABRACHIAL NUCLEAR COMPLEX

The parabrachial nuclear complex located in the dorsolateral pons from 4 to 3.1 mm posterior to the interaural plane, consists of three major subdivisions (the Kölliker-Fuse nucleus (KF) and medial and lateral parabrachial subfields). The medial (PBm) and lateral (PBl) subfields are further subdivided on the basis of projections and function (Chamberlin, 2004; Saper, 1995). Labeled neurons in these regions were mostly small round or fusiform cells, but KF also contained some larger multipolar cells. Additionally labeling in these nuclei was predominantly on the ipsilateral side with a few cells found contralaterally. 91.7% of labeled neurons in KF, 79.8% of labeled neurons in PBm, and 95.5% of labeled neurons in PBl were on the ipsilateral side. Figure 11 A-C compares the numbers of neurons in these nuclei in each animal between the ipsilateral and contralateral sides with bar graphs. In all animals except the

one with the earliest survival time (C53) labeled neurons were present in KF, PBm, and PBI (Table 1). KF was considerably infected within the *early* survival animals with numbers of labeled neurons ranging from 57 to 149, where as PBm and PBI had numbers of labeled neurons ranging from 11 to 50 and 1 to 8 respectively. KF still had the most infected neurons in the *intermediate* group with 177 to 302 labeled neurons as opposed to 92 to 159 infected neurons found in PBm and only 22 to 29 neurons infected in PBI. Within PBI infected neurons were scattered throughout the medial, dorsolateral, and lateral crescent areas. Figure 8 illustrates the pattern of infection in these nuclei by displaying maps of sections through this region from 3 different animals. Figure 8 also displays the morphology of labeled cells in these groups with photomicrographs from two *intermediate* cases.

OTHER MEDULLARY AND PONTINE NUCLEI

The spinal trigeminal nucleus (5SP) was labeled in all of the *intermediate* group animals with numbers of labeled neurons ranging from 11 to 60. The principle trigeminal nucleus (5P) was also labeled within the *intermediate* group but only in cases that had diencephalon labeling (C39 and C51). Numbers of labeled neurons in this region ranged from 9 to 20. The anteroventral (CVA) and dorsal (CD) cochlear nuclei each had a single labeled neuron between the two *intermediate* cases that had labeling in the diencephalon. More labeled neurons were found bilaterally in these regions and the posteroventral (CVP) cochlear nucleus only in the *late* survival group. Infected neurons in these regions were small round cells. The nucleus of the trapezoid body (NTB), located ventral to the superior olivary nucleus, was only labeled in the same animals, however, there were more labeled neurons in this region compared to the cochlear nuclei with 10 to 13 infected cells found within the two *intermediate* cases that had labeling in

the diencephalon. Infected neurons in NTB were medium or small multipolar or fusiform cells distributed bilaterally. Scattered neurons were also observed near the peripheral borders that may have been within the cuneate and gracile nuclei. The cuneate nucleus was sparsely labeled bilaterally within one animal from the *early* group (3 neurons) and within the *intermediate* survival group animals with 2 to 20 infected neurons. The gracile nucleus had just 2 infected neurons in one of the more advanced *intermediate* cases. Infected neurons in the cuneate nucleus were mostly medium or small fusiform cells and labeled neurons in the gracile nucleus were relatively smaller fusiform cells. In the *late* survival group many more neurons were infected in these areas. The locations of the trigeminal nuclei, cochlear nuclei and the cuneate and gracile nuclei are illustrated in Berman's cat brain atlas (Berman, 1968).

MIDBRAIN LABELING

None of the *early* group cases had infection in the midbrain, but all of the *intermediate* animals did. One animal in the *intermediate* group (C38) had infection in the midbrain but no farther rostral while the other two animals in this group (C51 and C39) had infection reach the diencephalon and cortex. In C38 infection was most pronounced within a dense group of medium or small multipolar and fusiform cells located in the lateral periaqueductal gray matter (IPAG). This area is a subdivision of the larger periaqueductal gray matter (PAG) that surrounds that cerebral aqueduct from 1.5 mm posterior to the interaural plane to 7.5 mm anterior from the interaural plane. The periphery of the PAG can be distinguished from surrounding areas by the fiber tracts that line its outside edge. Previous studies have identified several subdivisions of PAG including the dorsal (dPAG), dorsolateral (dIPAG), ventrolateral (vIPAG), and IPAG based on stimulations, projection pathways, lesions, c-FOS studies, and immunohistochemical

localization of chemical markers (Bandler et al., 2000; Ruiz-Torner et al., 2001). In the animal with infection restricted to the midbrain there were 83 infected neurons in IPAG and in the two animals with labeling in the diencephalon there was 227 and 458 labeled neurons in IPAG. This dense group of neurons was located in the ventral extent of the IPAG and may have overlapped into the vIPAG to some extent. There were also several medium or small multipolar and fusiform neurons labeled throughout the vIPAG in each of the *intermediate* group animals. There were 6 labeled neurons in the vIPAG in the case that only had midbrain infection (C38) and 56 to 90 infected neurons in the cases that had diencephalon labeling (C39 and C51). Additionally the dPAG contained smaller sized infected neurons in all *intermediate* cases with 1 labeled neuron in C38 and 48 to 111 infected neurons in C39 and C51 (Table 2). The dIPAG was the least labeled of the PAG subdivisions with only 2 to 6 neurons in the cases with diencephalon labeling (C39 and C51). In each of the subdivisions described above infection was bilateral. Figure 12 displays maps of sections through the PAG from the case with infection restricted to the midbrain (C38) and a case with diencephalon infection (C51) as well as photomicrographs of IPAG from two *intermediate* group cases.

The IPAG contained the most infected neurons in the midbrain of the animal with infection confined to the midbrain (C38) but in the two animals with diencephalic labeling (C39 and C51) more infected neurons were seen in the mesencephalic reticular nucleus (MRN). The MRN includes the paralemniscal and central tegmental fields illustrated in Berman's cat brain atlas from 2.1 mm posterior from the interaural plane to 6.4 mm anterior to the interaural plane (Berman, 1968). In C38 there was only 35 labeled neurons in MRN but in the two cases with diencephalon labeling there was 645 to 969 infected neurons in this region (Table 2). Infected cells in MRN were typically medium sized with some larger and smaller cells that were

multipolar or fusiform and distributed bilaterally. Figure 12 displays the pattern of infection in MRN with maps of sections from two *intermediate* group animals as well as the morphology of infected neurons in this region with a photomicrograph from an *intermediate* case.

The pedunculopontine (PP) and cuneiform nuclei (CN) also displayed several labeled neurons in each of the *intermediate* group animals. Previous studies that histochemically localized cholinergic neurons in the cat identified PP as a group of neurons surrounding the brachium conjunctivum in the the dorsolateral tegmentum from 2 mm posterior to the interaural plane to 1 mm anterior from the interaural plane (Jones and Beaudet, 1987). The cuneiform nucleus lying on the dorsal border of PP, is laterally bordered by the dorsal nucleus of the lateral lemniscus and medially bordered by the rostral extent of locus coeruleus and the caudal extent of PAG. CN spans from 2 to 0.9 mm posterior from the interaural plane (Berman, 1968). In the animal with labeling confined to the midbrain (C38), 5 and 9 neurons were labeled in CN and PP respectively. In the two *intermediate* group animals with infection in the diencephalon (C39 and C51) many more labeled neurons were seen in these areas with counts ranging from 14 to 56 in CN and 99 to 215 in PP (Table 2). Infected neurons in both regions were medium or small multipolar or fusiform cells distributed bilaterally. Figure 12 illustrates the infection in these regions with maps of sections from 2 *intermediate* group animals at different stages of infection.

Three other midbrain regions were labeled in all of the *intermediate* group cases. These regions were nucleus locus coeruleus (LC), Edinger-Westphal nucleus (EW), and the red nucleus (RN). In the cat LC extends from 4 to 0.9 mm posterior to the interaural plane. Caudally LC lines the lateral extent of the 4th ventricle and rostrally it is positioned ventrolaterally to the cerebral aqueduct, as illustrated in Berman's cat brain atlas (Berman, 1968). EW is located on the midline of the rostral midbrain, ventral to the PAG from 4.1 to 5.2 mm anterior to the

interaural plane. The RN is positioned in the rostral extent of the ventrolateral cat midbrain from 4.1 to 6.4 mm anterior to the interaural plane. This group of large cells is medially bordered by the oculomotor nerve. In the animal with infection confined to the midbrain 5, 6, and 1 infected neurons were found in LC, EW, and RN respectively. Within the two *intermediate* group animals that had diencephalon infection (C39 and C51) numbers of labeled neurons in LC, EW, and RN ranged from 19 to 44, 17 to 59, and 51 to 204 respectively (Table 2). Infected neurons in LC were medium or small multipolar and fusiform cells distributed bilaterally, infected neurons in EW were mostly medium sized multipolar cells, and infected neurons in RN were medium or large multipolar cells distributed with a strong contralateral predominance. The one RN neuron in C38 was on the contralateral side and in C39 and C51 84.3% and 91.2% of RN infection was on the contralateral side. Figure 11D illustrates the number of infected neurons in the RN on each side of the brain in the *intermediate* group animals with bar graphs. Figure 12 displays the pattern of infection in RN and LC with maps of sections from two *intermediate* group animals at different stages of infection. Figure 12 also shows the morphology of infected neurons in RN with a photomicrograph from an *intermediate* group animal.

Several additional areas of the midbrain were labeled exclusively within the two animals from the *intermediate* group that had labeling in the diencephalon (C39 and C51). These areas included the intermediate (SCI) and deep (SCD) layers of the superior colliculus. Positioned within the rostral tectum, the SCI and SCD lie dorsal and lateral to the PAG from 0.6 to 4.1 mm anterior from the interaural plane. In SCI numbers of labeled neurons ranged from 20 to 29 and in SCD they ranged from 13 to 33 (Table 2). Infected neurons in these regions were medium sized multipolar cells distributed bilaterally. The central nucleus of the inferior colliculus (ICC), positioned in the caudal tectum lateral to the PAG from 2.1 to 0.2 mm posterior from the

interaural plane was also labeled in C39 and C51. Three to four medium sized multipolar neurons were infected in ICC (Table 2). Finally, the nucleus of the posterior commissure (PCN) was also labeled in the two *intermediate* group animals with diencephalic infection (C39 and C51). PCN is located at the rostral extreme of the midbrain lateral to the posterior commissure, which is situated dorsal to the PAG, from 5.2 to 6.4 mm anterior from the interaural plane. Infected neurons in this region ranged from 13 to 14 small multipolar and fusiform cells. One additional midbrain region, the dorsal nucleus of the lateral lemniscus (LLDN) was only labeled in one of the *intermediate* cases (C51). Nine small, infected neurons were observed in this area. In the *late* group many more neurons were found bilaterally in each of these regions as well as in a few other midbrain regions including the dorsal raphe nucleus, external nucleus of the inferior colliculus, substantia nigra pars compacta, and substantia nigra pars reticulata.

DIENCEPHALON

The majority of infected neurons in the diencephalon were observed in the perifornical region (PerF). This area has been identified by studies that localized hypocretin containing neurons and has been defined as a group of cells within the dorsal, posterior and lateral hypothalamic areas concentrated dorsally and laterally from the fornix, including the region of the fields of Forel just ventral to zona incerta (Abrahamson and Moore, 2001; Zhang et al., 2002). Infection in PerF consisted of medium and small multipolar and fusiform cells distributed bilaterally. Numbers of infected neurons in PerF ranged from 108 to 148 in *intermediate* cases with many more neurons seen in this area in *late* cases. Figure 13 illustrates the pattern of infection in PerF with maps of sections from an *intermediate* animal (C51), as well as the morphology of labeled neurons in this region with a photomicrograph from a *late* case.

A few other areas in the diencephalon were also labeled within the *intermediate* group including the medial parvocellular division of the paraventricular nucleus of the hypothalamus (PVN) and intralaminar thalamic nuclei in the central lateral nucleus (CLN), ventrolateral nucleus of the thalamus (VL), and the paraventricular nucleus of the thalamus (PVT). The PVN is defined in Berman's cat atlas as a group of small cells extending laterally from the dorsal aspect of the third ventricle from 11 to 12 mm anterior from the interaural plane (Berman, 1968). Infected neurons in this region were small multipolar and fusiform cells distributed bilaterally. In *intermediate* animals numbers of infected neurons in PVN ranged from 17 to 34. Figure 13 illustrates the pattern of infection in PVN with maps of sections from an *intermediate* animal as well as the morphology of infected neurons in PVN with a photomicrograph from an *intermediate* case. The CLN is positioned within the thalamus lateral to the mediodorsal nucleus of the thalamus from 7.9 to 11 mm anterior to the interaural plane. In *intermediate* animals 17 to 18 small mostly multipolar neurons were found distributed bilaterally in this region. The VL is located in the lateral thalamus from 10.2 to 12 mm anterior to the interaural plane, as illustrated in Berman's cat brain atlas (Berman, 1968). Infected neurons in this region were mostly small multipolar cells that were distributed bilaterally. Numbers of infected neurons from the *intermediate* animals in VL ranged from 20 to 23. PVT, located lateral to the portion of the third ventricle coursing through the thalamus only presented 5 small multipolar or fusiform infected neurons in one of the *intermediate* animals. Additionally smaller multipolar infected neurons were observed in the central nucleus of the amygdala (ACE) in *intermediate* animals. This region is positioned lateral and ventral to the optic tract from 11 to 12.9 mm anterior to the interaural plane. The relative extent of infection in ACE was determined qualitatively. In animals from the *late* group all of the diencephalon areas described above showed increased

numbers of infected neurons distributed bilaterally.

CORTEX

Infection in the cortex was found bilaterally within two animals from the *intermediate* group (C39 and C51). Infected neurons were present within the deep lamina of the cruciate sulcus and within the prefrontal and insular cortices, which are defined in Scannell's review on the connectivity of the cat cerebral cortex (Scannell et al., 1995). In the *late* group increased numbers of neurons were found in these areas. Infected neurons in the cruciate sulcus were mostly medium pyramidal cells. Figure 14 illustrates these neurons with photomicrographs from an *intermediate* and a *late* case. Infected neurons in the prefrontal cortex were smaller round cells and infection in the insular cortex consisted of medium and small multipolar cells. The cruciate sulcus showed the most substantial amount of infection in the cortex in all cases considered. More specifically labeling was most concentrated in the pre-cruciate region of the sulcus, as illustrated in Figure 14.

DISCUSSION

INTRODUCTION

The results of this study have produced a number of findings that are novel to previous studies utilizing transneuronal tracing techniques from diaphragm circuitry. Several areas in the medulla and pons were identified to project to the diaphragm that have not been previously shown to be synaptically linked with the central circuits controlling diaphragm activity. Also, the deep cerebellar nuclei were shown to be synaptically linked to the circuitry controlling diaphragm activity, which has not been revealed by previous studies. In addition to finding novel regions in the brainstem, this study also identified higher order connections with diaphragm circuitry from regions of the midbrain, diencephalon, and cortex that have not been well described by previous transneuronal tracing studies. Interestingly, a number of these areas have been previously implicated in controlling behaviors that have respiratory components and thus projections from specific brain areas to the central circuits controlling diaphragm activity may be prescribed particular roles in modulating respiration. The following sections will outline the findings of this study with an emphasis on defining the function of projections to the diaphragm circuitry from specific groups throughout the neuraxis. Additionally a discussion of the results as they relate to the specific transneuronal tracing of circuits innervating the diaphragm with rabies virus will follow.

SPECIFICITY OF VIRUS TRANSPORT

Following rabies injections into the diaphragm, large infected neurons were present in the area of the C4-C6 spinal gray matter known to contain phrenic motoneurons in the cat (Berger et al., 1984; Cameron et al., 1983; Rikard-Bell and Bystrzycka, 1980). Furthermore, heavy infection was present in the regions of the brainstem containing the dorsal and ventral respiratory groups (Cohen, 1981; Connelly et al., 1992; Feldman, 1986). In the four animals where infection did not progress to the cerebral cortex, no infected neurons were observed in the intermediolateral cell column (IML) in the mid-thoracic spinal cord, suggesting that transneuronal passage of virus did not occur through the sympathetic nervous system. This finding is in accordance with previous observations that rabies virus preferentially infects somatic motoneurons (Lafon, 2005; Tang et al., 1999). Animals with more advanced infections that included cerebral cortex exhibited extensive infection in the thoracic spinal cord, such that it was impossible to directly rule out the possibility that sympathetic preganglionic neurons were labeled. However, within the brainstem of these animals, few neurons were infected in the region of the rostral ventrolateral medulla (subretrofacial nucleus) known to control muscle blood flow (Dampney and McAllen, 1988). In addition, parasympathetic preganglionic neurons in the dorsal motor nucleus of the vagus were not infected in any of the animals, suggesting that rabies virus did not leak from the diaphragm and infect the parasympathetic innervation of the adjacent viscera. Thus there is considerable evidence that rabies virus specifically moved through diaphragm motoneuron circuits.

Additionally the results of this study were consistent with the conclusion that rabies is specifically transported in the retrograde direction. As stated above infection in less advanced cases resulted in labeling of cell groups that are known to project to the diaphragm, and

furthermore the punctate pattern of viral antigen distribution observed in labeled neurons has been shown in studies that examined the transport properties of another retrograde tracer, pseudorabies virus, to be characteristic of retrograde transport (Card et al., 1995).

SPINAL CORD INFECTION

In all animals, numerous infected presumed interneurons were present outside the cluster of labeled cells in C4-C6 surmised to be phrenic motoneurons. These interneurons were distributed bilaterally throughout the cervical and upper thoracic spinal cord, and were predominantly observed in the ventral horn. In the early and intermediate infection cases, the presumed interneurons were most heavily concentrated near the segments containing diaphragm motoneurons. These data support electrophysiological evidence that propriospinal neurons in the upper cervical (Anker et al., 2006; Nakazono and Aoki, 1994) and thoracic (Bellingham, 1999) spinal cord as well as local circuit neurons (Bellingham and Lipski, 1990; Douse and Duffin, 1993) provide inputs to phrenic motoneurons. The present data clarify the locations of the interneurons that have the strongest and most direct connections with phrenic motoneurons. The relatively large numbers of interneurons labeled in the immediate vicinity of phrenic motoneurons in the early infection cases suggest that local interneurons play a particularly important role in controlling diaphragm activity. There has also been a controversy in the literature regarding the locations of upper cervical interneurons that make connections with phrenic motoneurons in the cat. Several studies have identified neurons with inspiratory-related activity in the intermediolateral part of the gray matter and adjacent white matter of the upper cervical segments (Aoki et al., 1980; Douse et al., 1992; Duffin and Hoskin, 1987; Hoskin and Duffin, 1987a; Hoskin et al., 1988; Lipski and Duffin, 1986; Nakazono and Aoki, 1994).

Although one study suggested that this neuronal population makes extensive direct connections with diaphragm motoneurons (Nakazono and Aoki, 1994), others have disputed the finding (Douse et al., 1992; Lipski and Duffin, 1986). Another study identified interneurons in the central portion of the C1-C2 ventral horn whose axons could be antidromically activated by microstimulation in the vicinity of diaphragm motoneurons (Anker et al., 2006). Because interneurons in the same locations described in the latter study were labeled in the early infection cases, it seems likely that propriospinal interneurons in the ventral horn of the upper cervical cord could provide direct inputs to diaphragm motoneurons.

Labeled cells were only present near the vicinity of the intermediolateral cell column (IML) in cases that had very advanced infections in the spinal cord, as well as intermediate to advanced infections throughout the neuraxis. The fact that there was clearly a lack of labeling in the IML in less advanced cases suggests that if cells in the IML were infected in the more advanced cases then they may project to phrenic motoneurons through polysynaptic circuits. Additionally differences in terminal field density between sympathetic and motor fibers innervating the diaphragm could account for the relative delay of potential infection in the IML compared to other spinal cord labeling.

INFECTION OF THE MEDULLARY RESPIRATORY GROUPS

The distribution of infected neurons throughout the DRG and VRG columns was consistent with the functional roles prescribed to the divisions within these groups. The majority of excitatory inspiratory neurons in these columns reside in the DRG and rVRG (Cohen, 1981), which were the most heavily labeled divisions of the medullary respiratory columns in all animals. These results are in accordance with the role of the diaphragm as the primary muscle of

inspiration. Additionally the cVRG, which is the main center of excitatory expiratory motoneurons in these columns (Arita et al., 1987), was the least infected of the respiratory column divisions in all animals. This observation is consistent with diaphragm function as well since this muscle only causes passive expiration via relaxation (Miller et al., 1997) making it unlikely for excitatory expiratory neurons that drive active expiration to innervate the diaphragm. Thus neurons in the cVRG were probably not infected via retrograde passage of rabies directly from phrenic motoneurons but rather through multisynaptic circuits, and since there is no evidence of the cVRG projecting axon collaterals within the medulla (Arita et al., 1987) its more likely that this group was infected via retrograde transport from spinal cord interneurons that innervate diaphragm motoneurons. In fact an anterograde tracing study utilizing tritiated amino acids showed that the cVRG and rVRG both project to neurons in the ventral horn of cervical and upper thoracic spinal cord (Feldman et al., 1985), consistent with the spinal cord labeling found in this study.

The BOT would be expected to be more infected than cVRG following injections of a retrograde tracer into the diaphragm muscle as it is capable of causing passive expiration via its inhibitory projections to phrenic motoneurons (Merrill and Fedorko, 1984). This region did in fact contain many more infected neurons than the cVRG in all animals, but it also contained less infected neurons than in DRG and rVRG in all cases. This is consistent with previous studies because the DRG and rVRG are primarily responsible for driving inspiration via contraction of the diaphragm while the BOT's activity has also been associated with coordinating activity in the medullary respiratory columns. In fact, studies have identified extensive inhibitory projections from the BOT to DRG, rVRG, and cVRG (Jiang and Lipski, 1990; Merrill et al., 1983). This would suggest that following injection of a transneuronal retrograde tracer into the diaphragm

infection of the BOT would be less extensive than infection in DRG and rVRG and as numbers of neurons increased in the latter groups infection would then increase in BOT via retrograde transport from DRG and rVRG to BOT.

Similarly, the pre-BOT has been implicated in playing more of a respiratory-modulating role in light of its extensive excitatory and inhibitory projections to the other divisions of the medullary respiratory groups (Ezure et al., 1989). Additionally, the pre-BOT has been implicated as a respiratory pacemaker center in slice preparation studies in neonatal rats (Smith et al., 1991) necessitating the extensive projections from this group to other areas in the medullary respiratory columns. As such, infection in this group would be expected to lag behind that of the other divisions of the respiratory groups that project more heavily to phrenic motoneurons in the spinal cord. This was seen to hold true as in the earliest case pre-BOT was the only division of the medullary respiratory groups devoid of infection, and in the 2nd least advanced case only the expiratory cVRG had fewer infected neurons. Only after the number of infected neurons greatly increased in the DRG and rVRG did infection of the pre-BOT surpass that of the BOT, and it never surpassed the number of labeled neurons in DRG or rVRG.

The morphology of infected neurons in the medullary respiratory groups was also consistent with the functional roles that have been prescribed to them. The DRG, cVRG, and rVRG are predominantly involved in controlling respiratory motoneurons in the spinal cord while the BOT and pre-BOT are primarily associated with modulating the respiratory signals sent from the other areas in the respiratory columns. Thus one could potentially expect the majority of cells in the former regions to be larger than cells in the BOT and pre-BOT regions as they would have greater cellular demands in order to support their long descending axons to the spinal cord.

RETROTRAPEZOID NUCLEUS AND CHEMORECEPTION

The RTN was first identified by a study that examined the projections to the ventral respiratory group via injection of the retrograde tracer horseradish peroxidase into the VRG (Smith et al., 1989). The RTN was demonstrated to have dense projections to the medullary respiratory groups and has since been implicated in a couple of different respiratory related functions. Lesions of the RTN in the cat were seen to decrease ventilatory output and CO₂ sensitivity (Nattie et al., 1991), suggesting that this area acts to increase respiration in response to CO₂ sensation. Presumably such a function would involve projections to medullary regions that activate the phrenic motoneurons, however, our data did not strongly support this assertion. Following injection of rabies virus into the diaphragm the RTN only contained 1 infected neuron in the most advanced of the *early* cases, and even in *intermediate* cases the number of infected neurons in this region was small compared to other areas. Thus it is more likely that RTN was infected through a higher number of synapses rather than directly projecting to medullary neurons that innervate the phrenic motoneurons. The RTN may increase respiration by directly innervating neurons in the medullary respiratory groups that drive muscles of respiration other than the diaphragm. A comparison of RTN labeling following injection of a transneuronal retrograde tracer into other muscles of inspiration with the results of our study may show that this is the case.

In addition to being defined as a central chemosensory area the RTN has been implicated as an expiratory rhythmogenic center that acts in concert with the rhythmogenic neurons in the pre-BOT to maintain normal ventilation (Feldman and Del Negro, 2006). If the RTN is a brain center devoted to expiration then it's not as surprising to see a lack of heavy infection in this region following injection of rabies virus into the diaphragm because the diaphragm muscle is

primarily devoted to inspiration.

Several other brain areas have been implicated in chemoreception in addition to the RTN including the dorsal and ventral respiratory groups, the caudal raphe nuclei, locus coeruleus, the fastigial nucleus, and the caudal hypothalamus (Horn and Waldrop, 1998; Nattie, 1999). As such these areas would be expected to have inputs to motoneurons controlling muscles of respiration. Our results would suggest that this is the case, as each of the above areas was infected following transneuronal retrograde tracing from the diaphragm. However, the mechanisms underlying how these nuclei contribute to chemoreception mediated by the diaphragm may be different. The caudal raphe nuclei were labeled in all cases except the one with labeling confined to the medullary respiratory groups suggesting that these nuclei may modulate diaphragm activity in response to chemosensory signal with direct inputs to the medullary respiratory group neurons that project to phrenic motoneurons. Locus coeruleus, the fastigial nucleus, and the caudal hypothalamus on the other hand were mostly only infected in *intermediate* cases suggesting that if they exert a chemosensory driven influence on diaphragm activity then it is done through a greater number of synapses. However, the latter nuclei are also located more rostrally in the neuraxis and as such it would take longer for virus to reach them than the caudal raphe nuclei.

APNEA

Apnea, or the absence of breathing, implies inhibition of the diaphragm muscle. Such inhibition of the diaphragm could be achieved by a number of different mechanisms including inhibition of the phrenic motoneurons via direct projections from the BOT, or from indirect inhibition of phrenic motoneurons via inhibitory projections from the BOT or pre-BOT to excitatory neurons in the DRG and rVRG that project to phrenic motoneurons, or by inhibitory

projections to phrenic motoneurons from other brain areas. The exact mechanism of how apnea is accomplished is not clear, but previous studies have provided some illumination into this matter by identifying areas involved in the production of apnea. Lesioning of the parabrachial nuclear complex in the rostral dorsolateral pons in combination with sectioning of the vagi causes prolonged bouts of inspiration (Alheid et al., 2004). Subsequent electrical and chemical stimulation and inhibition studies have defined functional subdivisions within the parabrachial nuclear complex such that a more ventral subset of this region has been found to be capable of producing apnea while the more dorsal lateral subdivision facilitates inspiration (Chamberlin, 2004; Chamberlin and Saper, 1994; Dutschmann and Herbert, 1996). These more ventral subdivisions include parts of the KF, PBm and the intertrigeminal region, the latter of which was not infected following injection of rabies virus into the diaphragm of the cat. KF and PBm, however, were considerably infected in all animals except for the one with infection confined to the medullary respiratory groups. These results suggest that KF and PBm may mediate diaphragm components of apnea while the intertrigeminal region may be responsible for components of apnea mediated by other muscles of respiration.

Other studies have supplemented these findings by identifying the sensory afferents responsible for the diving reflex and tracing the projections from these sensory afferents. The ethmoidal nerve, a branch of the trigeminal nerve, when stimulated produces cardiorespiratory responses consistent with the diving reflex, which includes apnea. Injection of the transneuronal anterograde tracer, herpes simplex virus-1 (strain 129), into the ethmoidal nerve of the muskrat resulted in the infection of several brain areas including the ventrolateral extent of the parabrachial nucleus, KF, the dorsal and ventral medullary respiratory columns, and additionally the ventral paratrigeminal region (Panneton et al., 2000). Our data suggests that this ventral

paratrigeminal region, like KF and PBm, may be mediating diaphragm components of apnea as this area was considerably infected in all cases except the least advanced case where infection was confined to the medullary respiratory groups.

POSTURAL ADJUSTMENT AND RESPIRATION

Changes in posture can affect the length of the diaphragm muscle leading to compensatory changes in respiratory muscle activity, and the neural regions that mediate these compensatory changes include the vestibular nuclei, fastigial nuclei, and the medial reticular formation (Yates et al., 2002). Stimulation of the vestibular nerve produces changes in phrenic nerve activity, but after lesioning the medial and inferior vestibular nuclei with the excitotoxin, kainic acid, vestibulo-respiratory reflexes are lost (Yates et al., 1993). This would suggest that the MVN and IVN would be the most prominently infected regions of the vestibular nuclei following injection of rabies virus into the diaphragm, however, while these nuclei were in fact infected the lateral vestibular nucleus showed the greatest number of infected neurons in almost all cases. This could be because of the dense projections that the LVN receives from the fastigial nucleus (Batton et al., 1977; Carleton and Carpenter, 1983). The fastigial nucleus has been shown through stimulation studies to have inhibitory and excitatory effects on respiration (Yates et al., 2002), and thus these effects could be mediated through projections to the LVN as well as by projections to the MRF. In fact previous studies involving stimulation of the LVN have suggested that this nucleus mediates excitatory and inhibitory modulations of respiration. The functional role of respiratory modulating neurons in the fastigial nucleus is not clear, but presumably they play a role in the compensatory changes of respiratory muscles associated with postural adjustments, since the fastigial nucleus does play a role in coordinating postural

adjustment. Additionally our results suggest that the IVN plays a more prominent role in vestibulo-respiratory reflexes than the MVN as the IVN was more infected than the MVN in every animal, and only the IVN was infected in *early* cases.

Respiratory signals from the vestibular nuclei have been shown to be mediated through neurons in the medial reticular formation. Firing in neurons of the MRF that were antidromically activated from the vicinity of diaphragm motoneurons were modulated by whole-body rotations in the vertical plane that stimulate vestibular receptors and by stimulation of the vestibular nerve (Wilkinson et al., 2004). These neurons were distributed bilaterally from the level of the obex to approximately 7 mm rostral to the obex, but they were most heavily concentrated at approximately 5 mm rostral to the obex. This is consistent with our study such that this was the most labeled part of the MRF in the majority of animals following injection of rabies into the diaphragm in the cat, suggesting that MRF neurons that relay vestibular signals to diaphragm motoneurons represent a considerable portion of the population of MRF neurons that influence diaphragm function.

VOMITING

Vomiting, or emesis, is a behavior that requires the coordinated action of the major respiratory muscles. There are two phases of vomiting termed retching and expulsion. During retching the diaphragm and abdominal muscles contract at the same time, likely to provide momentum to the bolus, and during expulsion the diaphragm relaxes and abdominal contractions are reinforced pushing the bolus out of the stomach and esophagus (Miller et al., 1997). The neural circuits mediating this process are not entirely clear but have been seen to involve the cVRG for the abdominal components during retching and expulsion (Miller et al., 1987), the

BOT for inhibition of the excitatory projections to phrenic motoneurons during expulsion (Miller and Nonaka, 1990; Miller et al., 1990), and neurons in the pre-BOT that are active during retching and have the capacity to inhibit neurons in BOT, DRG, rVRG, and cVRG (Miller and Ezure, 1992). Only a subset of these neurons in pre-BOT are active during vomiting, presumably so that only the BOT is inhibited allowing the coactivation of phrenic and abdominal muscles to take place via activity in DRG, rVRG, and cVRG. However, while this may be the case for cVRG, studies have shown that the neurons in DRG and rVRG that drive phrenic neuron activity are inhibited throughout vomiting (Miller et al., 1990). Thus it seems likely that there are additional areas of the brain that are essential for the production of emesis.

In fact, studies have implicated additional brain regions in the process of emesis. One study identified neurons near the medullary midline that are active during the coactivation of phrenic and abdominal activity (Miller et al., 1996). Additionally after lesioning these areas with injections of the excitotoxin kainic acid, the capacity to produce vomiting was eliminated or greatly attenuated in the cat. This suggests the involvement of medial reticular formation and/or caudal raphe neurons in the production of emesis. Our data are consistent with this hypothesis, since following injection of rabies into the diaphragm of the cat both of these cell groups were infected in all cases except the one where infection was only found in the medullary respiratory groups. The MRF was especially infected in our experiment and interestingly similar experiments in another emetic animal, the ferret, also showed an advanced infection in the MRF while in the non-emetic rat MRF infection was not as substantial (Dobbins and Feldman, 1994; Yates et al., 1999). Moreover, transneuronal retrograde tracing studies examining the inputs to phrenic and abdominal muscles identified neurons in the MRF that project to both of these muscles (Billig et al., 2000), consistent with the idea that neurons in this region may be

responsible for coactivation of these muscles during vomiting. These neurons were concentrated in the magnocellular division of the MRF in the ferret, which was also heavily infected in our experiment following injection of rabies virus into the diaphragm of the cat. Moreover, the vestibular nuclei have been implicated in the production of vomiting as inputs from this region have been shown to be capable of eliciting emesis (Grélot and Miller, 1994; Miller et al., 1996). Presumably the inputs from the vestibular nuclei to respiratory related MRF neurons are responsible for this observation.

LOCOMOTION AND RESPIRATION

In order to meet the metabolic demands imposed by locomotion, respiratory activity is accordingly increased. Chemoreceptor feedback mechanisms cannot entirely explain this phenomenon as blood gas and pH levels remain relatively unaltered during locomotion. Thereby, feedforward mechanisms are also thought to exist such that areas that promote locomotion also send collaterals to regions that control respiration (Waldrop et al., 1996). In fact, electrical or chemical stimulation of regions involved in the production of locomotion, like the mesencephalic locomotor region (MLR) or the hypothalamic locomotor region (HLR), simultaneously produce increases in respiratory activity in paralyzed ventilated preparations in which pulmonary and muscle afferents have been eliminated (Eldridge et al., 1981; Eldridge et al., 1985; Horn and Waldrop, 1998; Shik and Orlovskii, 1976; Waldrop et al., 1988). The results of our study are consistent with these findings in that the MLR, which is anatomically defined as the cuneiform and pedunculopontine nuclei, and the HLR, which is located in the posterior and lateral hypothalamic regions as well as adjacent areas including the Fields of Forel (Waldrop et al., 1996), were both infected following injection of rabies virus into the diaphragm of cats. The

location of the HLR is not very precisely defined, however, it seems to be consistent with the perifornical area that was considerably infected in our experiment. Other regions that were infected in our study have also been implicated in simultaneously producing locomotion and increased respiratory activity including the parapyramidal region, which is defined as the part of the MRF and raphe nuclei dorsal to the pyramids, and the lateral reticular nucleus (Ezure and Tanaka, 1997; Jordan et al., 2008). Additionally the substantia nigra, which was labeled in cases with advanced infections, is involved in the generation of movement and thus locomotion. This area was likely infected via its extensive connections with the pedunculopontine nucleus (Mena-Segovia et al., 2004).

RESPIRATION AND SLEEP

In general respiratory muscle activity is reduced during sleep compared to waking, however, diaphragm muscle activity is largely conserved compared to other respiratory muscles, consistent with its role as the muscle responsible for maintaining quiet breathing (Harding et al., 1986; Miller et al., 1997). Nevertheless, diaphragm activity is modified during sleep, especially in REM stages where its pattern of activity is highly irregular (Kline et al., 1986). These findings suggest that the central neural mechanisms controlling sleep/wake cycles have an influence on diaphragm function. As such, areas previously implicated in controlling sleep/wake states could potentially be infected following injection of rabies virus into the diaphragm. Many brain areas have been previously implicated in sleep/wake states, but infection of these areas following injection of rabies into the diaphragm was only seen in a subset of these nuclei including the locus coeruleus, midline raphe nuclei, pedunculopontine nucleus, and perifornical region. Neurons in these regions are all associated with arousal and are part of ascending arousal

pathways that project throughout the cortex (Saper et al., 2005). Some of these groups project through the intralaminar nuclei of the thalamus on their way to the cortex, perhaps explaining the infection we found in these regions in animals that had cortical infection. However, if sleep/wake related neurons were infected then they would presumably also have descending projections to explain infection in some of these groups in animals that did not have cortical labeling. Moreover, as detailed above, labeling in the PP and the perifornical area could be associated with the coupling of respiration and locomotion instead of sleep/wake regulation. However, serotonergic neurons in the raphe nuclei have been previously implicated in modulating the activity of respiratory group neurons that innervate phrenic motoneurons during sleep (Feldman and Smith, 1995) and the arousal related hypocretin neurons in the perifornical area have been shown to project to the ventral respiratory group as well as phrenic motoneurons. To more accurately determine whether sleep/wake related neurons were infected following injection of rabies virus into the diaphragm immunohistochemical analyses could be performed to verify the specific phenotypes of neurons in these groups.

RESPIRATORY COMPONENTS OF STRESS

The active defense reaction, physiologically characterized by tachypnea, tachycardia, and a redistribution of blood flow and behaviorally characterized by a “fight or flight” reaction, can be elicited by electrical or chemical stimulation of the midbrain PAG or the dorsomedial and posterior hypothalamic nuclei of the caudal hypothalamus (Bandler et al., 2000; Horn and Waldrop, 1998). Neurons in the caudal hypothalamus that control the respiratory component of this reaction, tachypnea, appear to overlap with the neurons that produce locomotion since stimulation in some of these areas can produce locomotion and defense reactions (Horn and

Waldrop, 1998). As was the case with the hypothalamic locomotor region, neurons in the caudal hypothalamus that produce a defense response may be consistent with infected neurons we observed within the perifornical region following injection of rabies virus into the diaphragm. Moreover, our results support previous studies that implicated the PAG in the production of respiratory-modulating defensive behavior as this area was considerably infected following injection of rabies virus into the diaphragm. However, the defense reactions that are mediated by the PAG are complex, and can be subdivided into “active” or “passive” coping strategies to stressors. The physiological and behavioral aspects of the “active” coping strategy are described above, and the “passive” coping strategy is physiologically characterized by bradypnea, bradycardia, and hypotension and behaviorally characterized by hyporeactivity and quiescence.

The different types of coping strategies that can be elicited from the PAG have been shown to be mediated by different subdivisions of the PAG. Electrical or chemical stimulation and c-FOS studies have implicated the lateral and dorsolateral regions of PAG in “active” coping and the ventrolateral division of PAG in “passive” coping (Bandler, 1982; Bandler and Carrive, 1988; Bandler and Keay, 1996; Bandler et al., 2000; Depaulis et al., 1994; Keay and Bandler, 1993; Keay et al., 1994). Presumably the descending projections from these regions influence the circuitry that innervates the respiratory muscles. In fact, the PAG has been found to project to areas that are known to influence respiration, like the parabrachial nuclei, the medial reticular formation, and throughout periaqueductal region which is analogous to the ventral respiratory column (Ennis et al., 1997; Mantyh, 1983). These studies found that the ventrolateral and lateral subdivisions of PAG projected heavily throughout the VRG while the dorsolateral division of PAG had few descending projections. Our results agree with these findings suggesting that the lateral and ventrolateral divisions of PAG mediate the respiratory components of “active” and

“passive” coping respectively. However, our results also reveal that the lateral PAG has a particularly strong influence on respiration as this area was the most heavily labeled of the PAG subdivisions in all cases. This could be because the respiratory aspects of “passive” coping are largely mediated by other respiratory muscles, or because “active” coping strategies have a much stronger influence on respiration compared to “passive” coping strategies.

Other brain areas, like the amygdala, have also been implicated in responses to stress. The amygdala has long been associated with defense reactions in the cat (Fernandez de Molina and Hunsperger, 1962). Moreover, the components of defense reactions elicited by the amygdala could be mediated by the extensive projections from the central nucleus of the amygdala to lateral, and ventrolateral subdivisions of the PAG (An et al., 1998; Rizvi et al., 1991). Our data are consistent with at least the respiratory components of stress reactions induced by the amygdala being mediated through the PAG as the central nucleus of the amygdala was infected in cases that had extensive infection in the PAG.

The paraventricular nucleus of the hypothalamus has also been implicated in reactions to stress. This nucleus has been shown to be a homeostatic center that integrates neuroendocrine and autonomic mechanisms that influence cardiorespiratory parameters (Swanson and Sawchenko, 1980). Stimulation of this nucleus with GABA antagonists or excitatory amino acids have revealed increased respiratory and diaphragm EMG activity (Schlenker et al., 2001; Yeh et al., 1997). Our data are consistent with these finding as we found infected neurons in the paraventricular nucleus of the hypothalamus following injection of rabies virus into the diaphragm. More specifically, labeled neurons were found in the parvocellular division of PVN which has been shown to have long descending projections to the brainstem and spinal cord (Swanson and Sawchenko, 1980).

Additionally the insular cortex is thought to play a role in emotion. This region is not well defined in the cat, however, it is believed to be a brain center that integrates a variety of sensory, motor, and limbic signals (Clascá et al., 1998). Infected neurons in this region could act to coordinate respiratory output signals with other sensory and limbic signals.

VOLUNTARY CONTROL OF RESPIRATION

Voluntary movements are controlled by the motor cortex, which in the cat is found within the cruciate sulcus (Keller, 1993; Scanell et al., 1995). Additionally the planning of these movements is influenced by neurons in the prefrontal cortex. As such, the neurons we found labeled in the cruciate sulcus and prefrontal cortex following injection of rabies virus into the diaphragm of cats were likely involved in the execution and planning of volitional respiratory muscle contractions. Moreover, within cases that had the least advanced cortical infection, infected neurons were most concentrated within the deep layers of the pre-cruciate region of the motor cortex, suggesting that this is the location of neurons that influence diaphragm function. Additionally infection that was observed in other areas of the brain following injection of rabies virus into the diaphragm could be explained as part of the pathway for voluntary execution of respiration. The red nucleus is known to be part of a descending pathway from the motor cortex (Hartmann von Monakow et al., 2004), and as such it is not surprising that we observed labeling in this region antecedent to infection in the cortex. Additionally, the dentate nucleus is involved in the coordination of voluntary movements, and as such infected neurons in this region may be involved with the coordination of respiration with other voluntary behaviors.

INFECTION IN VISUAL AND AUDITORY PATHWAYS

There were several regions that were labeled in this study following injection of rabies virus into the diaphragm that have not been previously implicated in respiration or behaviors that have respiratory components, interestingly, these regions included areas within the visual and auditory pathways. The intermediate and deep layers of the superior colliculus, which actually contained considerable numbers of infected neurons, are principally involved in producing saccadic eye movements but they are also responsive to mixed sensory modalities (Meredith and Stein, 1985). The observation of infection in the superior colliculus may imply that neurons in this region are coordinating respiratory activity with visual cues. This may be possible since certain visual cues can elicit changes in respiration. For example, seeing something that is alarming can cause an increase in respiratory activity. Along the same line of thought, an alarming auditory cue can cause changes in respiration, perhaps explaining the infection of neurons in the auditory-related inferior colliculus. The cochlear nuclei, dorsal nucleus of the lateral lemniscus, and the nucleus of the trapezoid body were logically labeled in more advanced cases as these nuclei project to the inferior colliculus. Similarly the nucleus of the posterior commissure was likely labeled in more advanced cases via its projections to the superior colliculus.

INFECTION IN DORSAL COLUMN NUCLEI

The dorsal column nuclei (cuneate and gracile nuclei), which relay touch and proprioceptive sensory signals, were also infected following injection of rabies into the diaphragm despite the fact that they have not been previously associated with respiratory muscle activity. However, these nuclei have been shown to project to other infected areas that have been

associated with respiratory muscle activity, such as the lateral PAG and cuneiform nucleus (Björkeland and Boivie, 1984), perhaps explaining their infection in our study.

CONCLUDING REMARKS

In addition to supporting the findings of previous studies employing transneuronal retrograde tracing techniques from diaphragm circuitry, this study provided new insight into the hierarchy of circuitry that influences contraction of the diaphragm muscle. Moreover, this study revealed that the circuits controlling diaphragm function are complex and highly integrated with the neural circuits that control a variety of other non-respiratory behaviors.

APPENDIX A: LIST OF ABBREVIATIONS

5P, principle trigeminal nucleus
5SP, spinal trigeminal nucleus
ACE, central nucleus of the amygdala
BC, brachium conjunctivum
BOT, Bötzing complex
dIPAG, dorsolateral periaqueductal gray matter
dPAG, dorsal periaqueductal gray matter
EW, Edinger-Westphal nucleus
CD, dorsal cochlear nucleus
CLN, central lateral nucleus of the thalamus
CN, cuneiform nucleus
CR, cruciate sulcus
CVA, anteroventral cochlear nucleus
CVP, posteroventral cochlear nucleus
cVRG, caudal ventral respiratory group
DRG, dorsal respiratory group
DRN, dorsal raphe nucleus
GR, gracile nucleus
ICC, central nucleus of the inferior colliculus
ICX, external nucleus of the inferior colliculus
IN, insular cortex
IVN, inferior vestibular nucleus
KF, Kölliker-Fuse nucleus
LC, nucleus locus coeruleus
LLDN, dorsal nucleus of the lateral lemniscus
IPAG, lateral periaqueductal gray matter
LRN, lateral reticular nucleus
LVN, lateral vestibular nucleus
medLRF, medullary lateral reticular formation
mNTS, medial nucleus of the solitary tract
MRF, medial reticular formation

MVN, medial vestibular nucleus
NC, cuneate nucleus
ND, dentate nucleus
ND, dentate nucleus
NI, interpositus nucleus
NTB, nucleus of the trapezoid body
PBI, lateral parabrachial nucleus
PBm, medial parabrachial nucleus
PCN, nucleus of the posterior commissure
PerF, perifornical area
ponLRF, pontine lateral reticular formation
PP, pedunculopontine nucleus
Pre-BOT, pre-Bötzing complex
PreF, prefrontal cortex
Pur, purkinje cell layer of cerebellar cortex
PVN, parvocellular division of the paraventricular nucleus of the hypothalamus
PVT, paraventricular nucleus of the thalamus
RN, red nucleus
RO, raphe obscurus
RP, raphe pallidus
RTN, retrotrapezoid nucleus
rVRG, rostral ventral respiratory group
SCD, deep layer of the superior colliculus
SCI, intermediate layer of the superior colliculus
SNc, substantia nigra pars compacta
SNr, substantia nigra pars reticulata
SVN, superior vestibular nucleus
v5SP, ventral paratrigeminal region
VL, ventrolateral nucleus of the thalamus
vIPAG, ventrolateral periaqueductal gray matter

APPENDIX B: TABLES AND FIGURES

Table 1: Total numbers of infected neurons counted bilaterally within infected areas of the medulla, pons and cerebellum. The check marks (✓) indicate the presence of infection as determined by qualitative analysis. Abbreviations are indicated in the list of abbreviations.

<i>Brain Area</i>	<i>Early Group</i>			<i>Intermediate Group</i>			<i>Late Group</i>	
	C53	C52	C21	C38	C39	C51	C36	C37
DRG	9	154	294	371	747	488	✓	✓
cVRG	1	25	85	101	181	81	✓	✓
rVRG	8	218	516	478	604	504	✓	✓
Pre-BOT	0	79	204	279	279	280	✓	✓
BOT	1	89	104	148	305	149	✓	✓
MRF	0	47	121	538	1570	1491	✓	✓
KF	0	57	149	183	302	177	✓	✓
PBm	0	11	50	143	159	92	✓	✓
PBI	0	8	1	29	29	22	✓	✓
mNTS	0	1	20	41	88	26	✓	✓
medLRF	0	84	297	554	1405	919	✓	✓
ponLRF	0	22	39	133	650	340	✓	✓
MVN	0	0	0	10	35	21	✓	✓
IVN	0	1	2	40	74	51	✓	✓
LVN	0	7	2	31	133	257	✓	✓
SVN	0	0	0	25	11	9	✓	✓
RTN	0	0	1	16	29	16	✓	✓
RP	0	2	1	15	43	16	✓	✓
RO	0	3	4	4	31	20	✓	✓
LRN	0	1	9	2	13	20	✓	✓
5SP	0	0	0	11	63	37	✓	✓
v5SP	0	26	38	48	99	68	✓	✓
5P	0	0	0	0	9	20	✓	✓
GR	0	0	0	0	0	2	✓	✓
NC	0	0	3	2	13	20	✓	✓
CD	0	0	0	0	1	0	✓	✓
CVA	0	0	0	0	0	1	✓	✓
CVP	0	0	0	0	0	0	✓	✓
NTB	0	0	0	0	10	13	✓	✓
NF	0	0	1	6	41	30	✓	✓
ND	0	0	1	1	9	24	✓	✓

Table 1 (continued)

NI	0	0	0	0	0	0	✓	✓
Pur	0	0	0	0	0	0	✓	✓

Table 2: Total number of infected neurons counted bilaterally within infected areas of the midbrain, diencephalon and cortex. Check marks (✓) indicate the presence of infection as determined by qualitative analysis. Abbreviations are indicated in the list of abbreviations.

<i>Brain Area</i>	<i>Intermediate Group</i>			<i>Late Group</i>	
	C38	C39	C51	C36	C37
dPAG	1	48	111	✓	✓
IPAG	83	458	227	✓	✓
vIPAG	6	56	90	✓	✓
dIPAG	0	2	6	✓	✓
EW	6	59	17	✓	✓
CN	5	56	14	✓	✓
PP	9	215	99	✓	✓
MRN	35	645	969	✓	✓
LC	5	44	19	✓	✓
RN	1	51	204	✓	✓
ICC	0	3	4	✓	✓
ICX	0	0	0	✓	✓
LLDN	0	0	9	✓	✓
SCI	0	29	20	✓	✓
SCD	0	33	13	✓	✓
PCN	0	13	14	✓	✓
DRN	0	0	0	✓	✓
SNc	0	0	0	✓	✓
SNr	0	0	0	✓	✓
PerF	0	108	148	✓	✓
PVN	0	17	34	✓	✓
CLN	0	18	17	✓	✓
PVT	0	5	0	✓	✓
VL	0	20	23	✓	✓
ACE	0	✓	✓	✓	✓
IN	0	✓	✓	✓	✓
CR	0	✓	✓	✓	✓
PreF	0	✓	✓	✓	✓

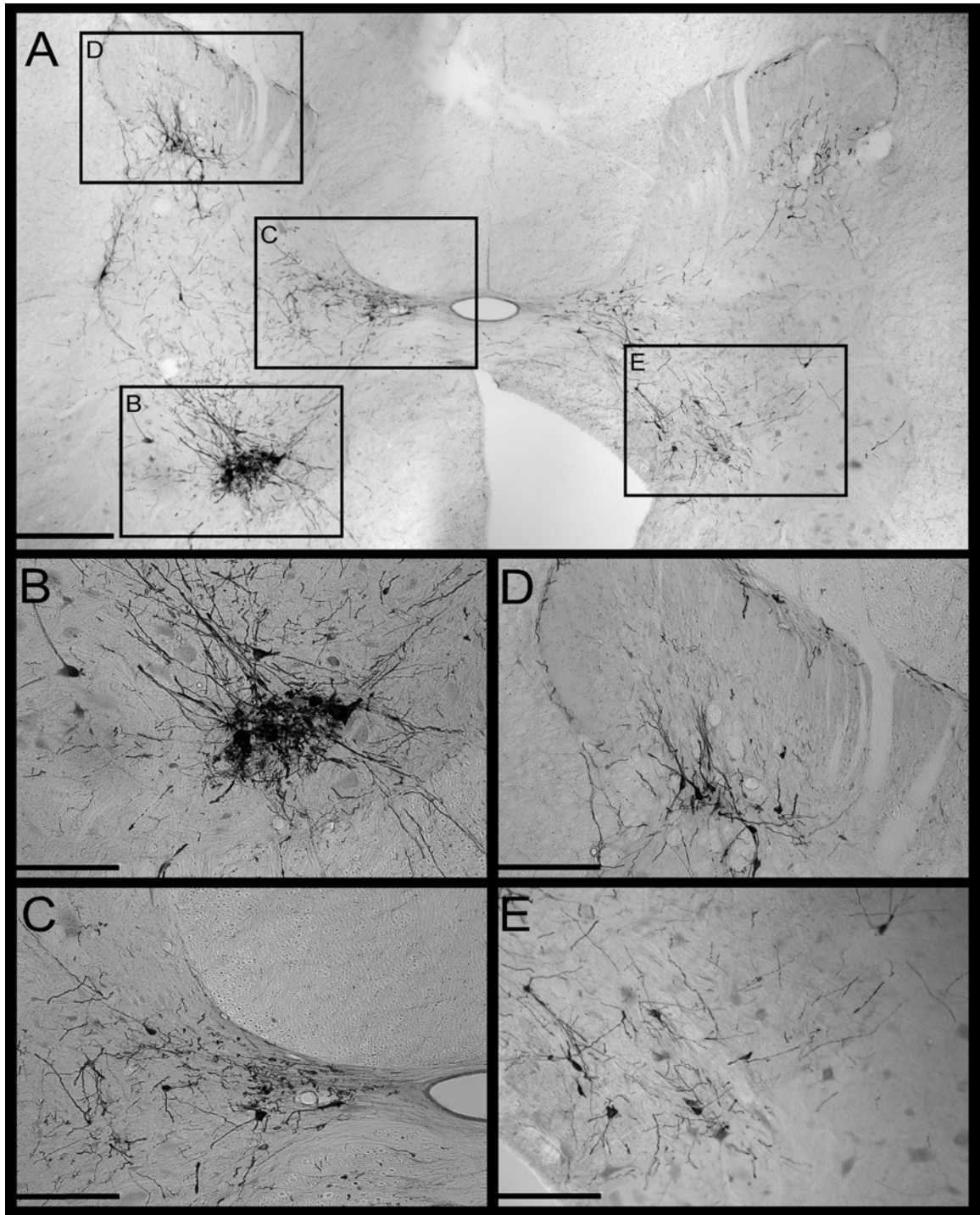


Figure 1: Photomicrographs of infected neurons in the C5 spinal cord of animal C21. A: photomontage of the entire C5 spinal gray matter of one section. Boxes denote regions depicted at higher magnification in subsequent panels. The left side of the section is ipsilateral to the rabies injections into the diaphragm. B: a dense cluster of presumed motoneurons in the ventral horn. C: A group of infected presumed interneurons in Rexed's lamina X and the medial portion of lamina VII. D: A group of infected presumed interneurons concentrated in Rexed's lamina V. E: Infected presumed interneurons in medial lamina VII and lamina VIII contralateral to the side of injections. Bars designate 500 μ m in panel A and 250 μ m in the other panels.

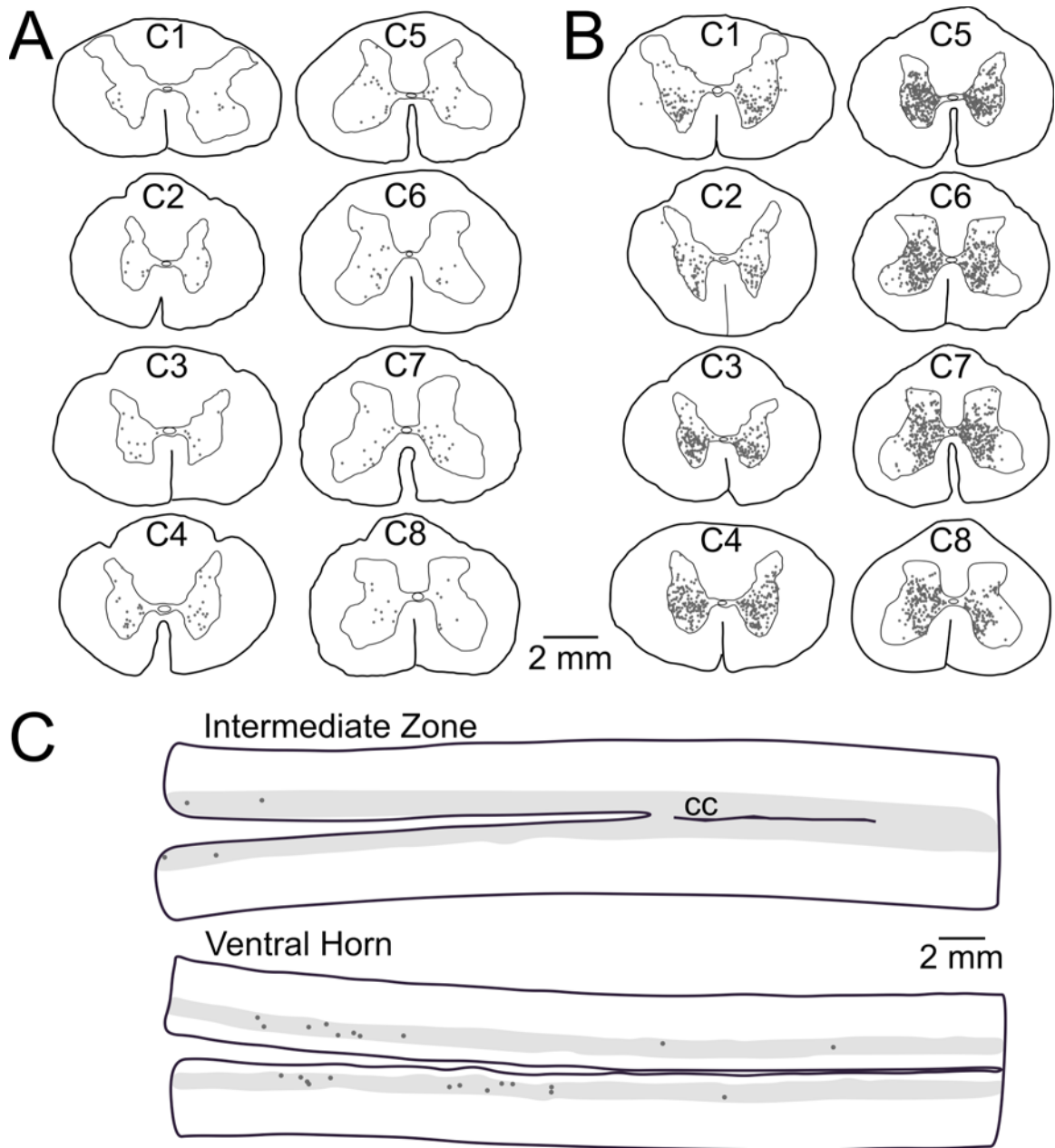


Figure 2: Locations of presumed interneurons labeled following the injection of rabies virus into the diaphragm. A and B: locations of labeled cervical interneurons in an early infection (animal C21, panel A) and an intermediate infection (animal C51, panel B) case. Representative transverse sections from each cervical segment are shown; the level is indicated on the section. C: locations of labeled interneurons in horizontal sections through the T5-T9 thoracic spinal cord of intermediate infection case C38. The gray matter is indicated as a shaded area, and the rostral end of the sections is towards the left side. The top section is through the intermediate zone, the portions of Rexed's lamina VII and X near the level of the central canal (CC). The bottom section is through the ventral horn. No sections that were clearly through the dorsal horn contained any infected neurons, and thus are not provided.

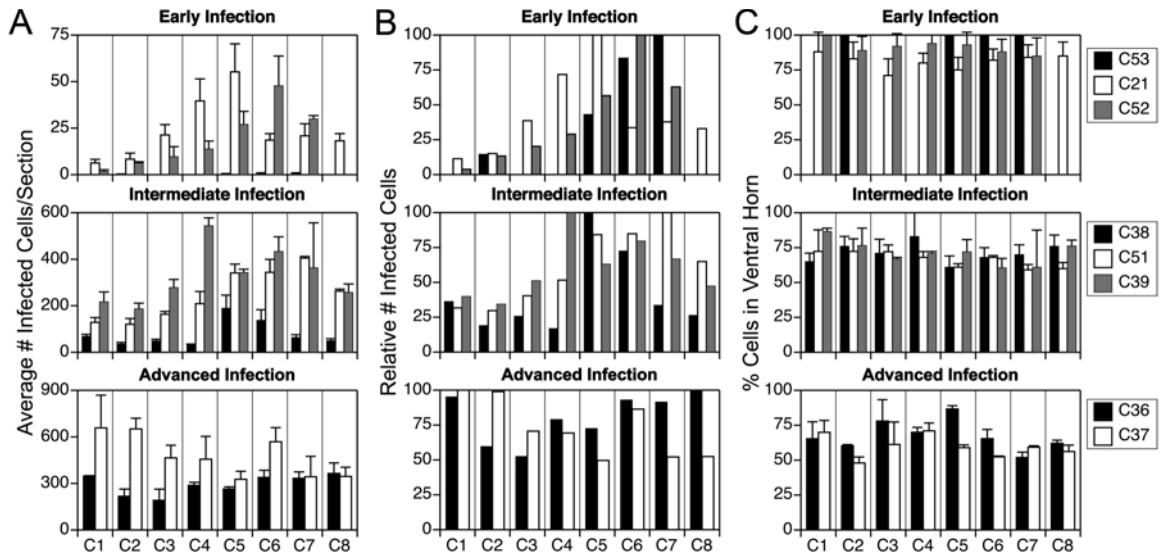


Figure 3: A: Histograms illustrating the average number of infected presumed interneurons per section in each cervical spinal cord segment. The C8 segment was not processed for case C52. Error bars indicate one standard deviation. B: The average cell count per section from panel A expressed relative to the maximal value obtained for any cervical segment in a particular animal (i.e., the segment with the maximal average number of interneurons per section is indicated as having a 100% relative infection). C: The average percentage of infected presumed interneurons per section that was located in the ventral horn (Rexed's laminae VII-X) in each cervical spinal cord segment. Error bars indicate one standard deviation.



Figure 4: Photomicrograph at 40X magnification of a medial reticular formation neuron in the *intermediate* animal C51 that illustrates the distribution of viral antigen within infected neurons. Note the homogeneous distribution of immunoreactivity within the cytoplasm as well as the punctate staining typically observed on the soma and dendrites of a rabies infected neuron.

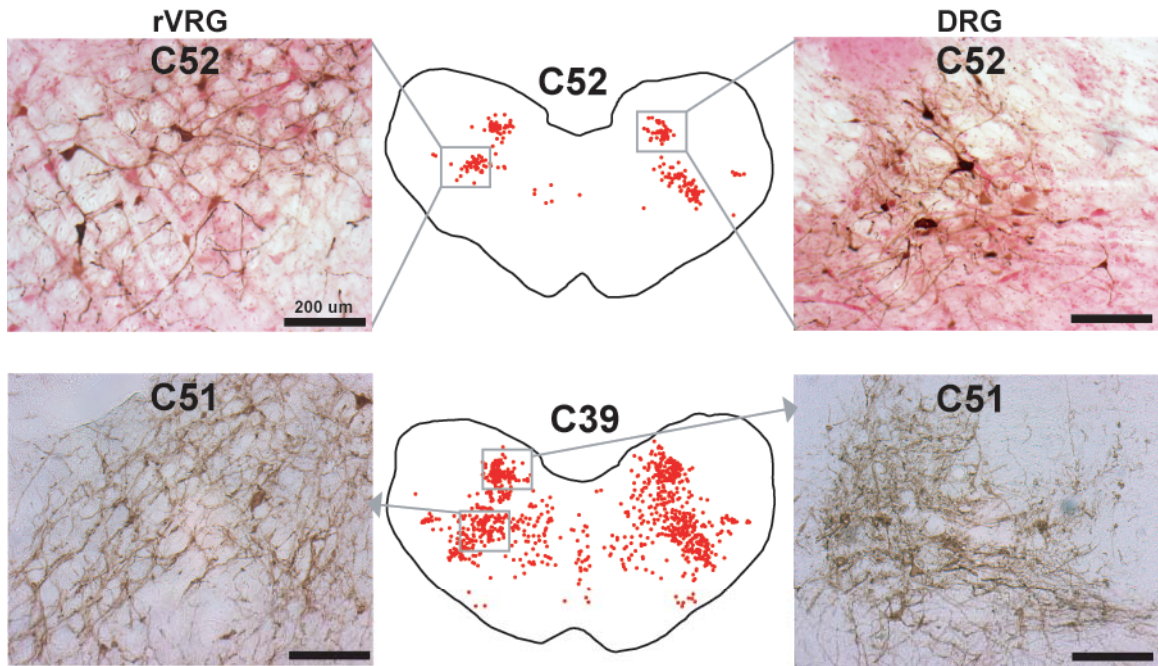


Figure 5: Maps of sections from an *early* (C52) and an *intermediate* (C39) case illustrating the localization of rabies infected neurons within the medulla 12.1 mm posterior to the interaural plane. Each dot in the maps represents a single labeled neuron. The dorsal respiratory group and the rostral ventral respiratory group are within the boxes in each map. Photomicrographs illustrate the morphology and distribution of labeled cells in these regions from an *early* (C52) and an *intermediate* (C51) case. The photomicrographs connected to boxes in the maps by two lines were taken from the same section used to create the map. Photomicrographs connected to boxes by a single line with an arrowhead are from an analogous case. All photomicrographs were taken at 10X magnification and the scale bars in each photomicrograph represent 200 μm .

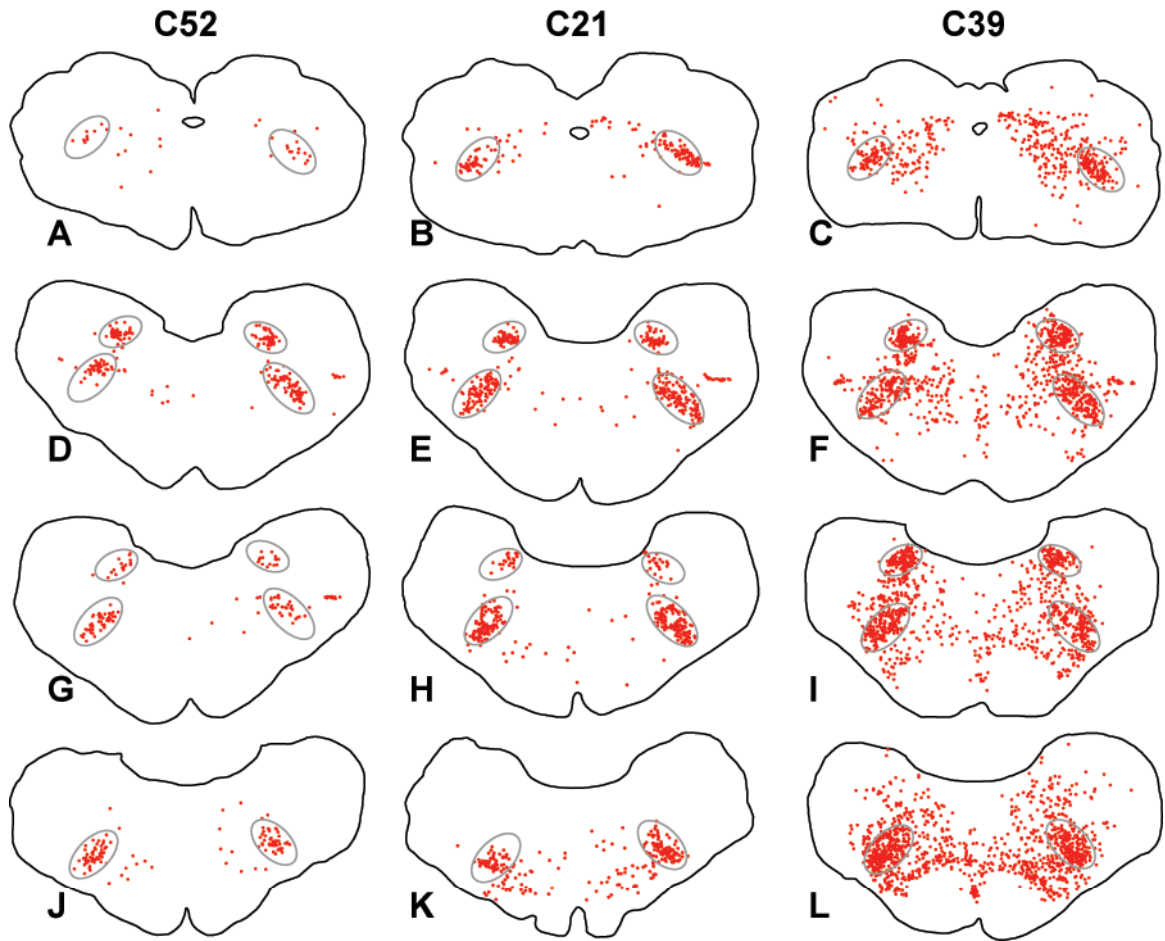


Figure 6: Maps of sections through the dorsal and ventral respiratory columns in two *early* (C52 and C21) cases and one intermediate (C39) case. Each dot represents a single infected neuron. The dorsal (DRG) and ventral (VRG) respiratory columns are depicted with the ovals drawn on each map. A-C illustrate the caudal VRG at 16 mm posterior from the interaural plane, D-F illustrate the DRG and the rostral VRG at 12.1 mm posterior from the interaural plane, G-I illustrate the DRG and pre-botzinger complex at 11.6 mm posterior from the interaural plane, and J-L illustrate the Botzinger complex at 10 mm posterior from the interaural plane.

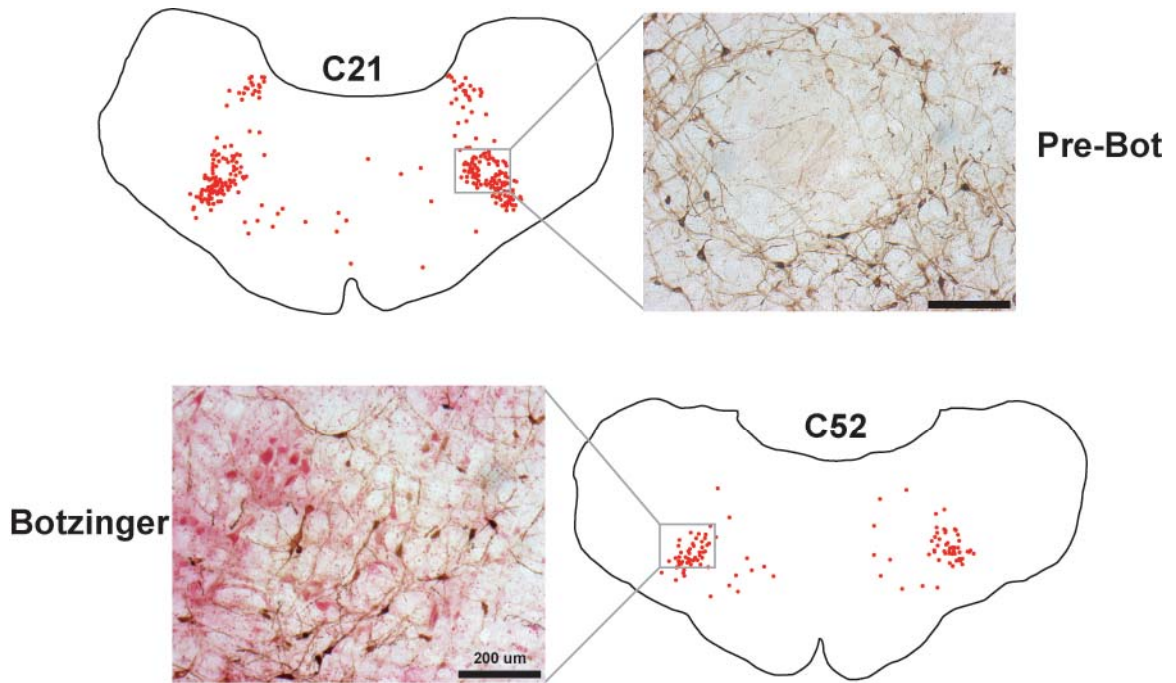


Figure 7: Maps and photomicrographs illustrating the distribution and morphology of infected neurons in the regions of pre-Bötzinger and Bötzing complex. Photomicrographs were taken at 10X magnification from the same sections used to create the corresponding maps. Pre-Bötzinger maps and photomicrographs are from a section located 11.6 mm posterior to the interaural plane, and Bötzing maps and photos are from a section located 10 mm posterior to the interaural plane. Scale bars in both photomicrographs represent 200 μm . Each dot on the maps represents a single infected neuron.

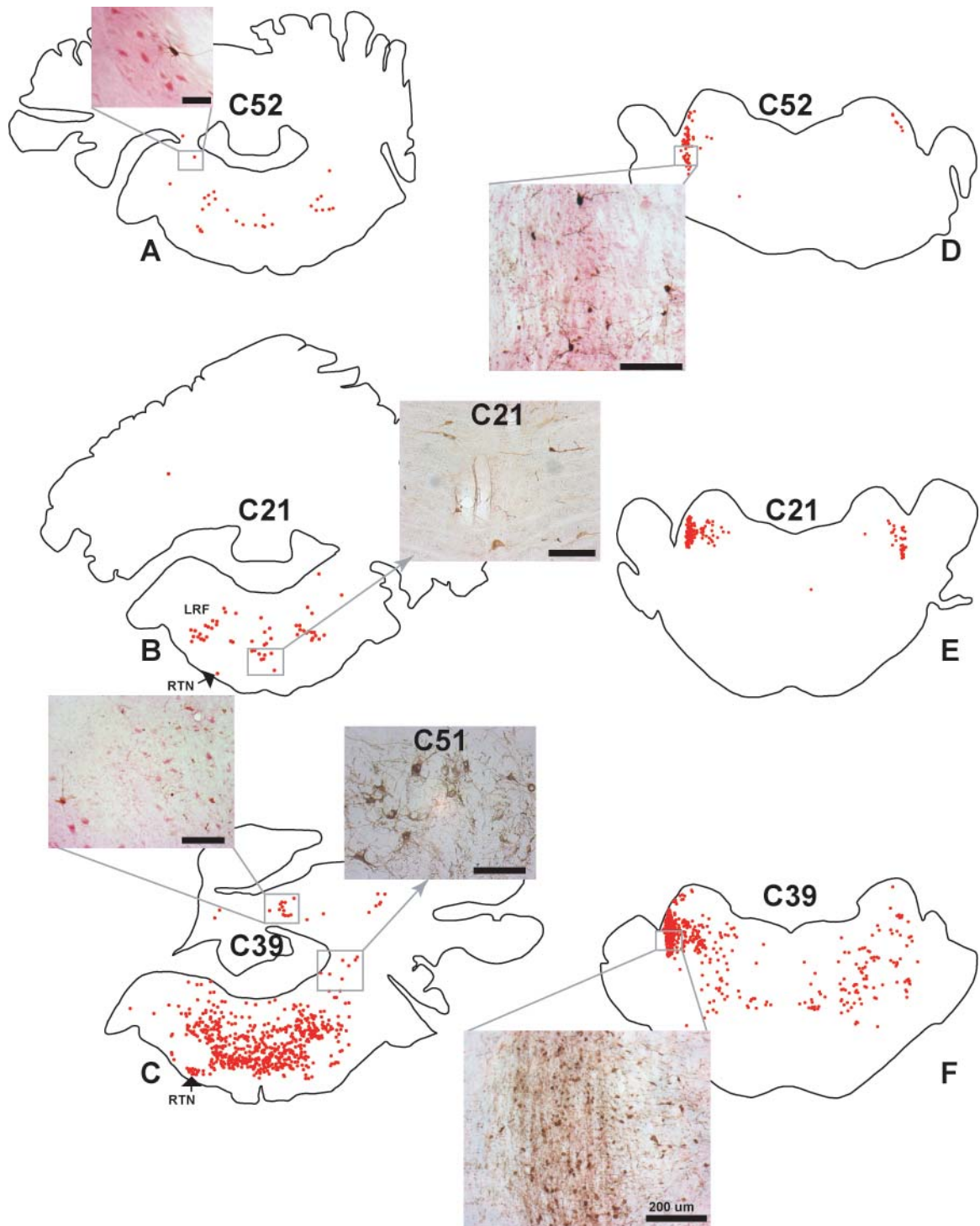


Figure 8: Maps of sections from two *early* (C52 and C21) and an *intermediate* (C39) case displaying the distribution of infected neurons in the rostral medulla and pons. A-C are located at 8.5 mm posterior to the interaural plane and D-F are located at 3.1 mm posterior to the interaural plane. Each dot represents a single labeled neuron. Photomicrograph in A illustrates an infected lateral vestibular nucleus neuron, the photomicrograph in B displays the labeled neurons in the medial reticular formation, the photomicrographs in C present infected neurons in the fastigial and lateral vestibular nuclei. The Kölliker-Fuse nucleus is illustrated in the photomicrographs in D and F. All photomicrographs were taken at 10X and scale bars represent 200 μm .

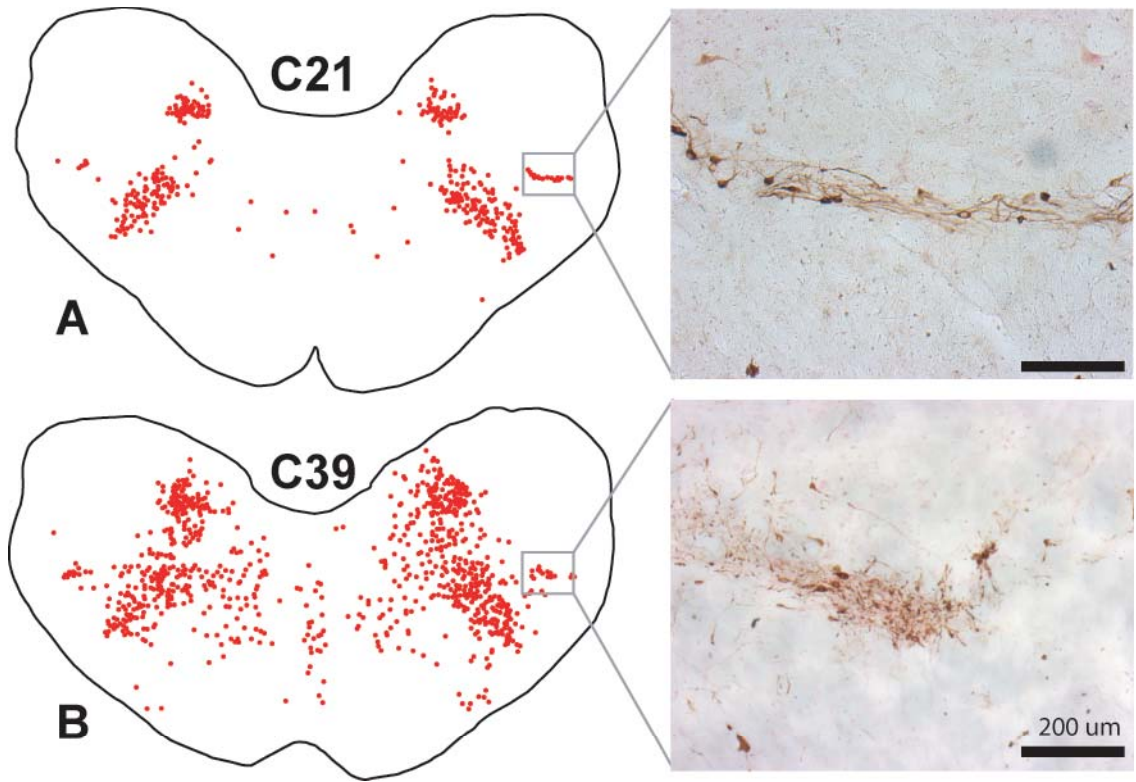


Figure 9: Maps and photomicrographs from an *early* (C21) and an *intermediate* (C39) case depicting the distribution and morphology of infected neurons in the ventral paratrigeminal nucleus. Photomicrographs are from the same sections used to create maps. Both photomicrographs were taken at 10X magnification and both scale bars represent 200 μm .

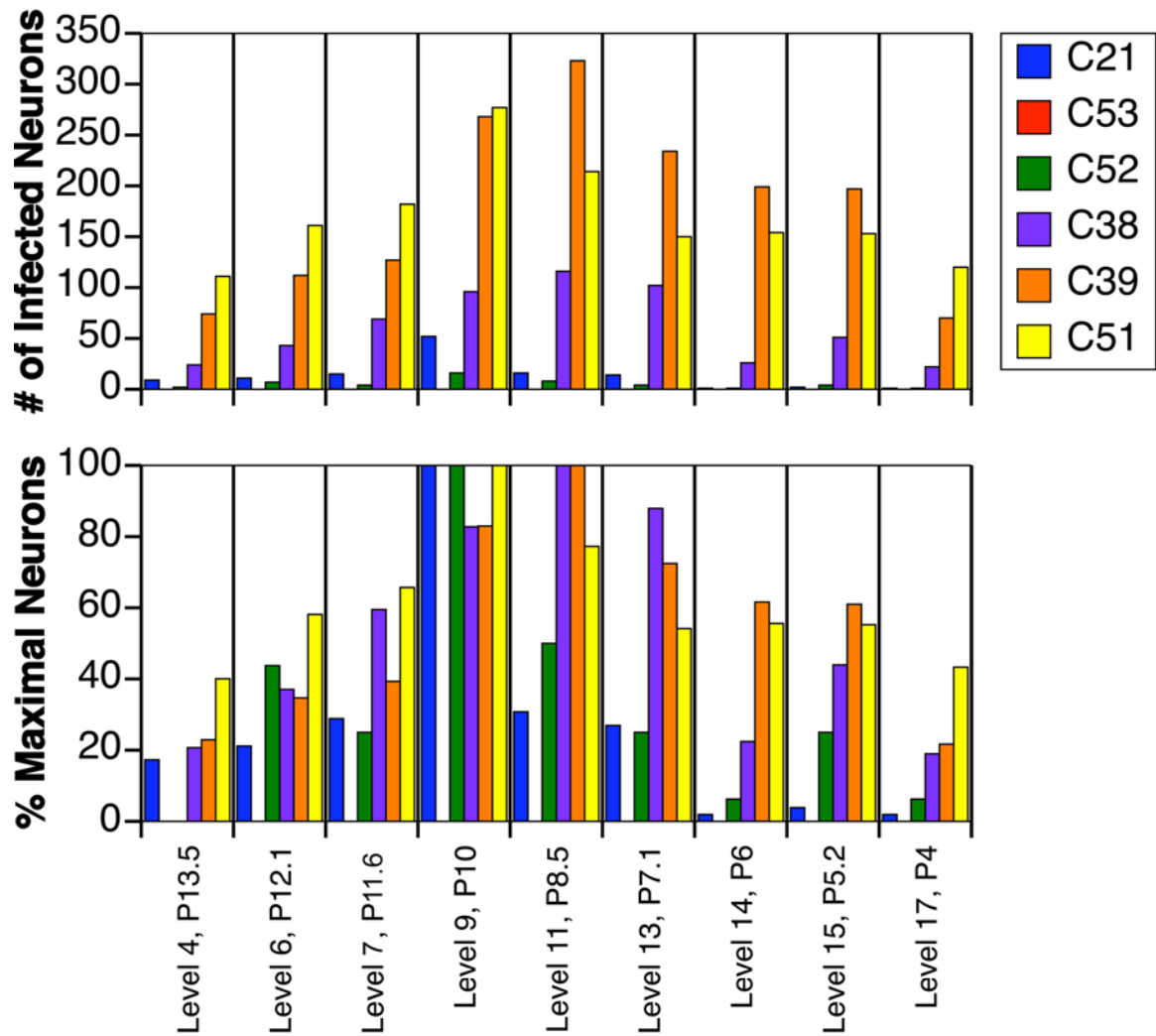


Figure 10: The top histogram displays the number of infected neurons at nine different levels throughout the medial reticular formation in each animal. The bottom panel displays the percentage of infected neurons at each level of the medial reticular formation relative to the number of neurons at the maximally infected level. The distance of each level posterior to the interaural plane is indicated in mm.

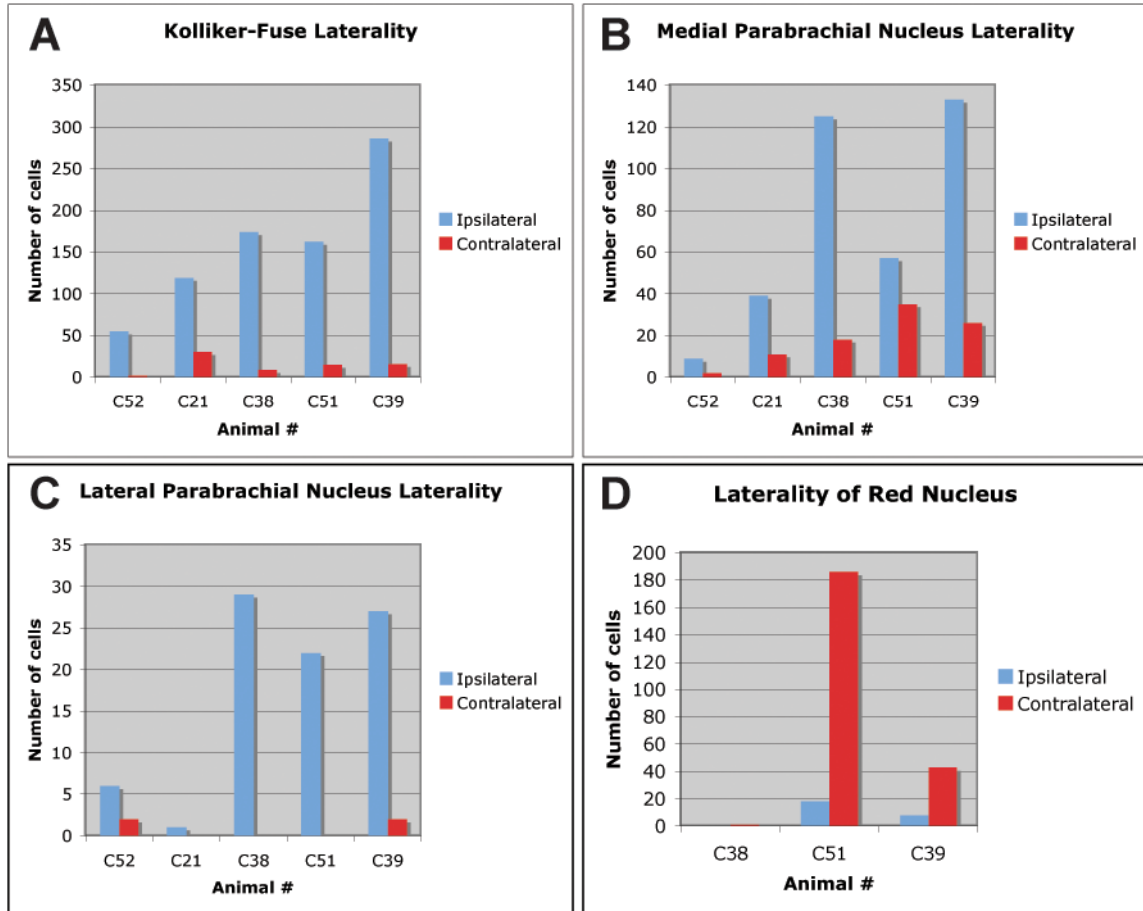


Figure 11: A: Total number of infected neurons in the Kölliker-Fuse nucleus counted on the ipsilateral and contralateral sides of the brain in each animal. B: The total number of infected neurons counted in the medial parabrachial nucleus on ipsilateral and contralateral sides of the brain in each animal. C: The total number of infected neurons counted on the ipsilateral and contralateral sides of the lateral parabrachial nucleus in each animal. D: Total number of infected neurons in the red nucleus on the ipsilateral and contralateral sides of the brain in each animal with red nucleus infection.

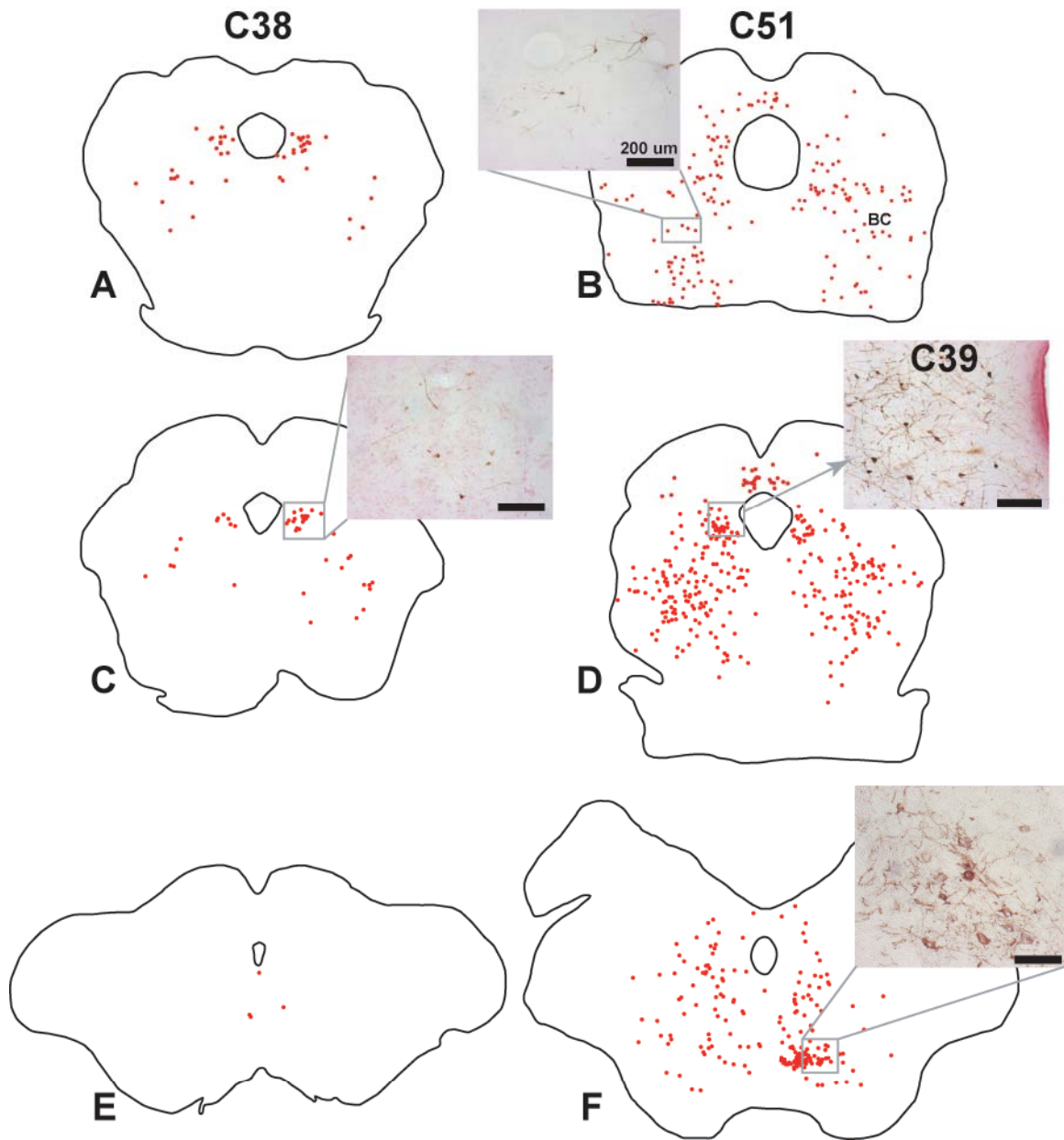


Figure 12: Maps of sections through the midbrain from two *intermediate* animals at different stages of infection (C38 and C51). A-B are located at 0.6 mm posterior to the interaural plane, C-D are located at 1.6 mm anterior to the interaural plane, and E-F are located 5.2 mm anterior to the interaural plane. The photomicrograph in B illustrates the morphology of infected neurons in the mesencephalic reticular nucleus, the photomicrographs in C and D depict the morphology of infected neurons in the lateral periaqueductal gray matter, and the photomicrograph in F depicts the morphology of infected neurons in the red nucleus. Photomicrographs connected to the corresponding boxed brain area in a map with two lines are taken from the same section used to create the map. Photomicrographs connected to the boxed brain areas with a single line are from an analogous section in a different animal. Each dot in the maps represents a single infected neuron and each photomicrograph was taken at 10X magnification. All scale bars represent 200 μm .

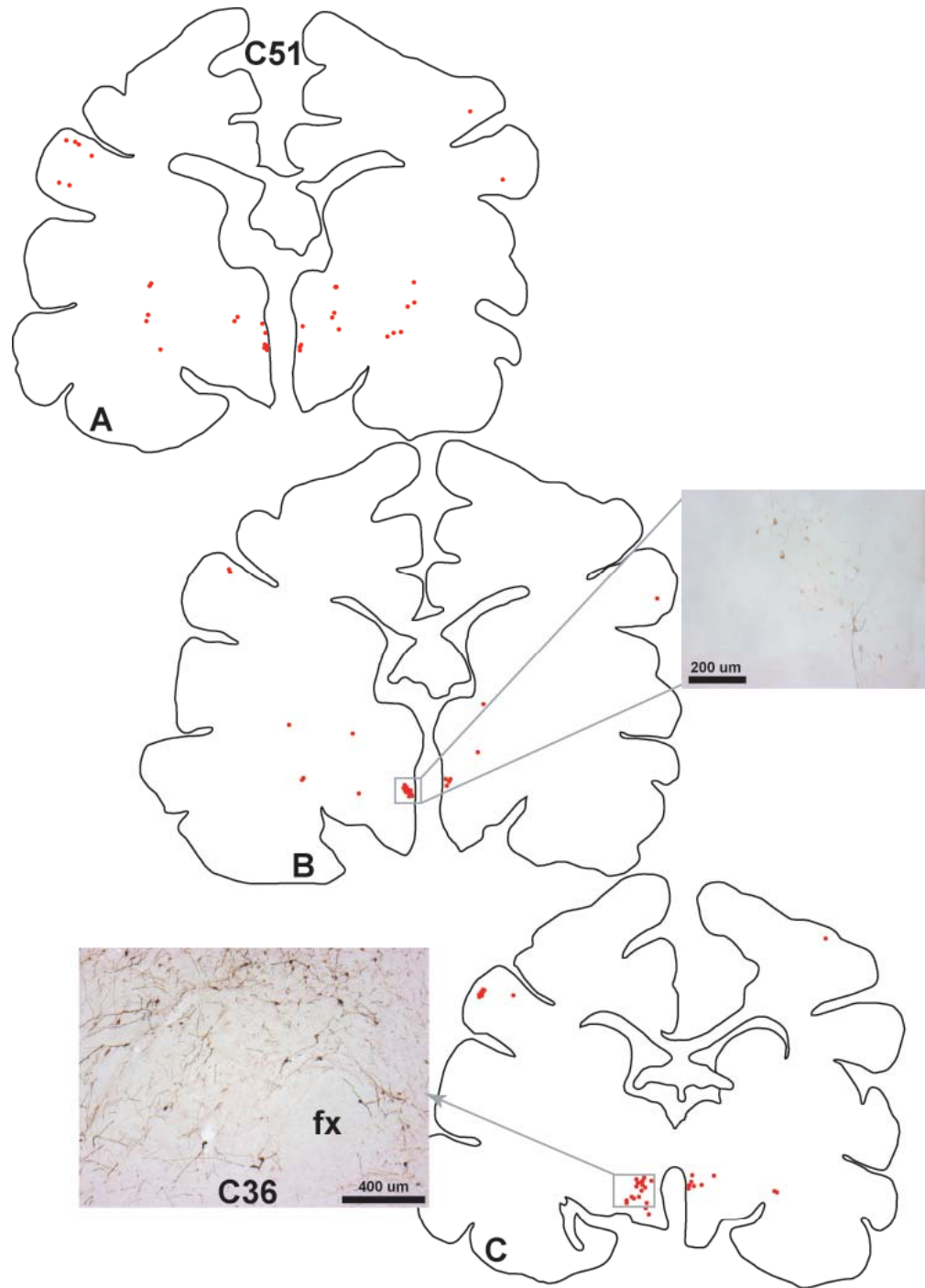


Figure 13: Maps of sections through the diencephalon from an *intermediate* case (C51). The section mapped in A is located at 11 mm anterior to the interaural plane, the map in B is from a section located 11.8 mm anterior to the interaural plane, and the section mapped in C is 12 mm anterior to the interaural plane. The photomicrograph in B was taken at 10X magnification from the same section used to create the corresponding map and illustrates the morphology of infected neurons in the parvocellular division of the paraventricular nucleus of the hypothalamus. The photomicrograph in C was taken at 5X magnification and depicts the morphology of labeled neurons in the perifornical area from a *late* case (C36). Apparent differences in the laterality of infection in maps of sections is due to the angle at which the tissue was cut. Infected neurons were distributed bilaterally in labeled areas within these maps.

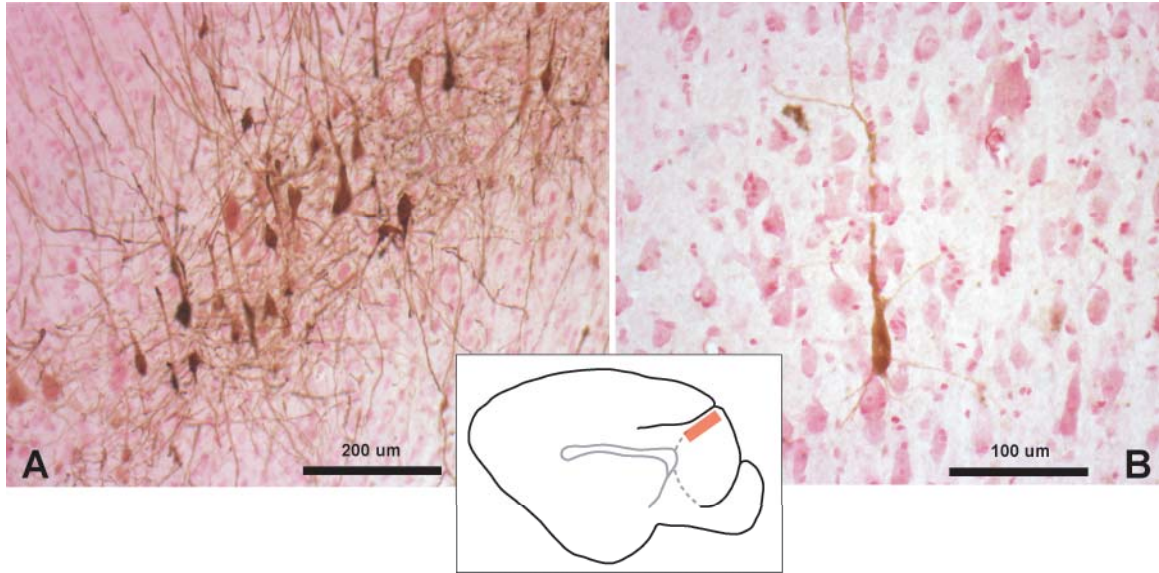


Figure 14: Photomicrographs of the cruciate sulcus from a *late* (C36) and an *intermediate* (C39) animal. Both photomicrographs were taken in the portion of the cruciate sulcus depicted in the schematic situated between the photos. The photomicrograph in A was taken at 10X and it illustrates the morphology of infected neurons in the cruciate sulcus from a *late* case. The photomicrograph in B was taken at 20X and depicts the morphology of a single neuron in the cruciate sulcus from an *intermediate* case.

BIBLIOGRAPHY

- Abrahamson EE, Moore RY. 2001. The posterior hypothalamic area: chemoarchitecture and afferent connections. *Brain Res* 889:1-22.
- Alheid GF, Milsom WK, McCrimmon DR. 2004. Pontine influences on breathing: an overview. *Respir Physiol & Neurobiol* 143:105-114.
- An X, Bandler R, Ongur D, Price JL. 1998. Prefrontal Cortical Projections to Longitudinal Columns in the Midbrain Periaqueductal Gray in Macaque Monkeys. *J Comp Neurol* 401:455-479.
- Anker AR, Sadacca BF, Yates BJ. 2006. Vestibular inputs to propriospinal interneurons in the feline C1-C2 spinal cord projecting to the C5-C6 ventral horn. *Exp Brain Res* 170(1):39-51.
- Aoki M, Mori S, Kawahara K, Watanabe H, Ebata N. 1980. Generation of spontaneous respiratory rhythm in high spinal cats. *Brain Res* 202(1):51-63.
- Arita H, Kogo N, Koshiya N. 1987. Morphological and physiological properties of caudal medullary expiratory neurons of the cat. *Brain Res* 401:258-266.
- Bandler R. 1982. Induction of rage following microinjections of glutamate in midbrain but not hypothalamus of cats. *Neurosci Lett* 30:183-188.
- Bandler R, Carrive P. 1988. Integrated defence reaction elicited by excitatory amino acid microinjection in the midbrain periaqueductal grey region of the unrestrained cat. *Brain Res* 439(1-2):95-106.
- Bandler R, Keay KA. 1996. Columnar organization in the midbrain periaqueductal gray and the integration of emotional expression. In: Holstege G, Bandler R, Saper CB, editors. *Emotional Motor System*. Sara Burgerhartstraat 25, PO Box 211, 1000 AE Amsterdam, Netherlands: Elsevier Science Publ B V. p 285-300.
- Bandler R, Keay KA, Floyd N, Price J. 2000. Central circuits mediating patterned autonomic activity during active vs. passive emotional coping. *Brain Res Bull* 53(1):95-104.
- Batton RR, 3rd, Jayaraman A, Ruggiero D, Carpenter MB. 1977. Fastigial efferent projections in the monkey: an autoradiographic study. *J Comp Neurol* 174(2):281-305.
- Bellingham MC. 1999. Synaptic inhibition of cat phrenic motoneurons by internal intercostal nerve stimulation. *J Neurophysiol* 82(3):1224-1232.
- Bellingham MC, Lipski J. 1990. Respiratory interneurons in the C5 segment of the spinal cord of the cat. *Brain Res* 533(1):141-146.
- Berger AJ. 1977. Dorsal respiratory group neurons in the medulla of the cat: spinal projections, responses to lung inflation and superior laryngeal nerve stimulation. *Brain Res* 135:231-254.
- Berger AJ, Cameron WE, Averill DB, Kramis RC, Binder MD. 1984. Spatial distributions of phrenic and medial gastrocnemius motoneurons in the cat spinal cord. *Exp Neurol* 86(3):559-575.

- Berman AI. 1968. *The Brain Stem of the Cat*. Madison: University of Wisconsin Press.
- Billig I, Foris JM, Enquist LW, Card JP, Yates BJ. 2000. Definition of neuronal circuitry controlling the activity of phrenic and abdominal motoneurons in the ferret using recombinant strains of pseudorabies virus. *J Neurosci* 20(19):7446-7454.
- Björkeland M, Boivie J. 1984. An anatomical study of the projections from the dorsal column nuclei to the midbrain in cat. *Anat Embryol (Berl)* 170(1):29-43.
- Cameron WE, Averill DB, Berger AJ. 1983. Morphology of cat phrenic motoneurons as revealed by intracellular injection of horseradish peroxidase. *J Comp Neurol* 219(1):70-80.
- Card JP. 1995. Pseudorabies virus replication and assembly in rodent CNS. In: Kaplitt MG, Loewy AD, editors. *Viral Vectors: Tools for Study and Genetic Manipulation of the Nervous System*. San Diego: Academic Press. p 319-347.
- Card JP, Dubin JR, Whealy ME, Enquist LW. 1995. Influence of infectious dose upon productive replication and transynaptic passage of pseudorabies virus in rat central nervous system. *J Neurovirol* 1(5-6):349-358.
- Card JP, Enquist LW, Miller AD, Yates BJ. 1997. Differential tropism of pseudorabies virus for sensory neurons in the cat. *J Neurovirol* 3(1):49-61.
- Carleton SC, Carpenter MB. 1983. Afferent and efferent connections of the medial, inferior and lateral vestibular nuclei in the cat and monkey. *Brain Res* 278(1983):29-51.
- Chamberlin NL. 2004. Functional organization of the parabrachial complex and intertrigeminal region in the control of breathing. *Respir Physiol & Neurobiol* 143:115-125.
- Chamberlin NL, Saper CB. 1994. Topographic organization of respiratory responses to glutamate microstimulation of the parabrachial nucleus in the rat. *J Neurosci* 14:6500-6510.
- Clascá F, Llamas A, Reinoso-Suárez F. 1998. Insular cortex and neighboring fields in the cat: A redefinition based on cortical microarchitecture and connections with the thalamus. *J Comp Neurol* 384(3):456-482.
- Cohen MI. 1979. Neurogenesis of Respiratory Rhythm in the Mammal. *Physiol Rev* 59(4):1105-1160.
- Cohen MI. 1981. Central determinants of respiratory rhythm. *Ann Rev Physiol* 43:91-104.
- Connelly CA, Dobbins EG, Feldman JL. 1992. Pre-Bötzinger complex in cats: respiratory neuronal discharge patterns. *Brain Res* 590:337-340.
- Dampney RAL, McAllen RM. 1988. Differential control of sympathetic fibres supplying hindlimb skin and muscle by subretrofacial neurones in the cat. *J Physiol* 395:41-56.
- Davies JGM, Kirkwood PA, Sears TA. 1985. The distribution of monosynaptic connexions from inspiratory bulbospinal neurones to inspiratory motoneurons in the cat. *J Physiol* 368:63-87.
- Depaulis A, Keay KA, Bandler R. 1994. Quiescence and hyporeactivity evoked by activation of cell bodies in the ventrolateral midbrain periaqueductal gray of the rat. *Exp Brain Res* 99:75-83.
- Dobbins EG, Feldman JL. 1994. Brainstem network controlling descending drive to phrenic motoneurons in rat. *J Comp Neurol* 347(1):64-86.
- Douse MA, Duffin J. 1993. Axonal Projections and Synaptic Connections of C5 Segment Expiratory Interneurons in the Cat. *J Physiol - London* 470:431-444.

- Douse MA, Duffin J, Brooks D, Fedorko L. 1992. Role of upper cervical inspiratory neurons studied by cross-correlation in the cat. *Exp Brain Res* 90(1):153-162.
- Duffin J, Hoskin RW. 1987. Intracellular recordings from upper cervical inspiratory neurons in the cat. *Brain Res* 435(1-2):351-354.
- Dutschmann M, Herbert H. 1996. The Kölliker-Fuse nucleus mediates the trigeminally induced apnoea in the rat. *Neuro Rep* 7:1432-1436.
- Eldridge FL, Gill-Kumar P, Millhorn DE, Waldrop TG. 1981. Spinal inhibition of phrenic motoneurons by stimulation of afferents from peripheral muscles. *J Physiol* 311:67-79.
- Eldridge FL, Millhorn DE, Kiley JP, Waldrop TG. 1985. Stimulation by central command of locomotion, respiration and circulation during exercise. *Respir Physiol* 59(3):313-337.
- Ennis M, Xu SJ, Rizvi TA. 1997. Discrete subregions of the rat midbrain periaqueductal gray project to nucleus ambiguus and the periambigual region. *Neurosci* 80(3):829-845.
- Ezure K. 1990. Synaptic connections between medullary respiratory neurons and considerations on the genesis of respiratory rhythm. *Prog Neurobiol* 35:429-450.
- Ezure K. 1996. Respiratory control. In: Yates BJ, Miller AD, editors. *Vestibular Autonomic Regulation*. Boca Raton, FL: CRC Press. p 53-84.
- Ezure K, Manabe M, Otake K. 1989. Excitation and inhibition of medullary inspiratory neurons by two types of burst inspiratory neurons in the cat. *Neurosci Lett* 104:303.
- Ezure K, Tanaka I. 1997. Convergence of central respiratory and locomotor rhythms onto single neurons of the lateral reticular nucleus. *Exp Brain Res* 113(2):230-242.
- Fedorko L, Merrill EG, Lipski J. 1983. Two descending medullary inspiratory pathways to phrenic motoneurons. *Neurosci Lett* 43:285-291.
- Fedorko L, Merrill EG. 1984. Axonal projections from the rostral expiratory neurones of the Bötzing complex to medulla and spinal cord in the cat. *J Physiol* 350:487-496.
- Feldman JL. 1986. Neurophysiology of breathing in mammals. In: Bloom FE, editor. *Handbook of Physiology The Nervous System, IV Intrinsic Regulatory Systems of the Brain*. Bethesda, MD: Am Physiol Soc. p 463-524.
- Feldman JL, Del Negro CA. 2006. Looking for inspiration: new perspectives on respiratory rhythm. *Nat Rev Neurosci* 7:232-242.
- Feldman JL, Loewy AD, Speck DF. 1985. Projection from the Ventral Respiratory Group to Phrenic and Intercostal Motoneurons in Cat: An Autoradiographic Study. *J Neurosci* 5(8):1993-2000.
- Feldman JL, Smith JC. 1995. Neural control of respiratory pattern in mammals: an overview. Dempsey JA, Pack A, editors. New York: Marcel Dekker.
- Fernandez de Molina A, Hunsperger RW. 1962. Organization of the subcortical system governing defence and flight reaction in the cat. *J Physiol* 160:200-213.
- Finke S, Conzelmann K. 2005. Replication strategies of rabies virus. *Virus Res* 111:120-131.

- Gaytán SP, Pásaro R, Coulon P, Bevengut M, Hilaire G. 2002. Identification of central nervous system neurons innervating the respiratory muscles of the mouse: A transneuronal tracing study. *Brain Res Bull* 57:335-339.
- Grélot L, Miller AD. 1994. Vomiting - its ins and outs. *News Physiol Sci* 9:142-147.
- Haber E, Kohn KW, Ngai SH, Holaday DA, Wang SC. 1957. Localization of Spontaneous Respiratory Neuronal Activities in the Medulla Oblongata of the Cat: A New Location of the Expiratory Center. *Am J Physiol* 190(2):350-355.
- Harding R, England SJ, Stradling JR, Kozar LF, Phillipson EA. 1986. Respiratory activity of laryngeal muscles in awake and sleeping dogs. *Respir Physiol* 66:316.
- Hartmann von Monakow K, Akert K, Künzle H. 2004. Projections of precentral and premotor cortex to the red nucleus and other midbrain areas in macaca fascicularis. *Exp Brain Res* 34(1):91-105.
- Holstege G. 1989. Anatomical study of the final common pathway for vocalization in the cat. *J Comp Neurol* 284(2):242-252.
- Horn EM, Waldrop TG. 1998. Suprapontine control of respiration. *Respir Physiol* 114(3):201-211.
- Hoskin R, Duffin J. 1987a. Excitation of upper cervical inspiratory neurons by inspiratory neurons of the nucleus tractus solitarius in the cat. *Exp Neurol* 95(1):126-141.
- Hoskin RW, Duffin J. 1987b. Excitation of upper cervical inspiratory neurons by inspiratory neurons of the nucleus retroambigualis in the cat. *Exp Neurol* 98(2):404-417.
- Hoskin RW, Fedorko LM, Duffin J. 1988. Projections from upper cervical inspiratory neurons to thoracic and lumbar expiratory motor nuclei in the cat. *Exp Neurol* 99(3):544-555.
- Hsu SM, Raine L, Fanger H. 1981. Use of avidin-biotin-peroxidase complex (ABC) in immunoperoxidase techniques: a comparison between ABC and unlabeled antibody (PAP) procedures. *J Hist Cyto* 29(4):577-580.
- Iscoe S. 1981. Respiratory and stepping frequencies in conscious exercising cats. *J Appl Physiol* 51:835-839.
- Jiang C, Lipski J. 1990. Extensive monosynaptic inhibition of ventral respiratory group neurons by augmenting neurons in the Bötzing complex in the cat. *Exp Brain Res* 81(3):639-648.
- Jones BE, Beaudet A. 1987. Distribution of Acetylcholine and Catecholamine Neurons in the Cat Brainstem: A Choline Acetyltransferase and Tyrosine Hydroxylase Immunohistochemical Study. *J Comp Neurol* 261:15-32.
- Jordan LM, Liu J, Hedlund PB, Akay T, Pearson KG. 2008. Descending command systems for the initiation of locomotion in mammals. *Brain Res* 57:183-191.
- Kalia M, Feldman JL, Cohen MI. 1979. Afferent projections to the inspiratory neuronal region of the ventrolateral nucleus of the tractus solitarius in the cat. *Brain Res* 171(1):135-141.
- Kawahara K, Kumagai S, Nakazono Y, Miyamoto Y. 1989. Coupling between respiratory and stepping rhythms during locomotion in decerebrate cats. *J Appl Physiol* 67:110-115.
- Keay KA, Bandler R. 1993. Deep and superficial noxious stimulation increases Fos-like immunoreactivity in different regions of the midbrain periaqueductal gray. *Neurosci Lett* 154:23-26.

- Keay KA, Clement CI, Oowler B, Depaulis A, Bandler R. 1994. Convergence of deep somatic and visceral nociceptive information onto a discrete ventrolateral midbrain periaqueductal gray region. *Neurosci* 61:727-732.
- Keller A. 1993. Intrinsic connections between representation zones in the cat motor cortex. *Neuro Rep* 4:515-518.
- Kelly RM, Strick PL. 2000. Rabies as a transneuronal tracer of circuits in the central nervous system. *J Neurosci Methods* 103:63-71.
- Kline L, Hendricks J, Davies R, Pack A. 1986. Control of the activity of the diaphragm in rapid-eye-movement sleep. *J Appl Physiol* 61:1293-1300.
- Lafon M. 2005. Rabies virus receptors. *J Neurovirol* 11(1):82-87.
- Lindsey BG, Segers LS, Morris KF, Hernandez YM, Saporta S, Shannon R. 1994. Distributed actions and dynamic associations in respiratory-related neuronal assemblies of the ventrolateral medulla and brain stem midline: evidence from spike train analysis. *J Neurophysiol* 72(4):1830-1851.
- Lipski J, Duffin J. 1986. An electrophysiological investigation of propriospinal inspiratory neurons in the upper cervical cord of the cat. *Exp Brain Res* 61(3):625-637.
- Lipski J, Merrill EG. 1980. Electrophysiological demonstration of the projection from expiratory neurones in rostral medulla to contralateral dorsal respiratory group. *Brain Res* 197:521-524.
- Loewy AD, Burton H. 1978. Nuclei of the solitary tract: efferent projections to the lower brain stem and spinal cord of the cat. *J Comp Neurol* 181:421-450.
- Mantyh PW. 1983. Connections of the Midbrain Periaqueductal Gray in the Monkey. II. Descending Efferent Projections. *J Neurophysiol* 49(3):582-594.
- McLean IW, Nakane PK. 1974. Periodate-lysine-paraformaldehyde for immunoelectron microscopy. *J Hist Cyto* 22:1077-1083.
- Mena-Segovia J, Bolam JP, Magill PJ. 2004. Pedunculopontine nucleus and basal ganglia: distant relatives or part of the same family? *TINS* 27(10):585-588.
- Meredith MA, Stein BE. 1985. Descending efferents from the superior colliculus relay integrated multisensory information. *Science* 227:657-659.
- Merrill EG. 1981. Where are the *real* respiratory neurones? *Fed Proc* 40:2389-2394.
- Merrill EG, Fedorko L. 1984. Monosynaptic inhibition of phrenic motoneurons: a long descending projection from Bötzing complex neurons. *J Neurosci* 4:2350-2353.
- Merrill EG, Lipski J. J. 1987. Inputs to Intercostal Motoneurons From Ventrolateral Medullary Respiratory Neurons in the Cat. *J Neurophysiol* 27:1837-1853.
- Merrill EG, Lipski J, Kubin L, Fedorko L. 1983. Origin of the expiratory inhibition of the nucleus tractus solitarius inspiratory neurones. *Brain Res* 263:43-50.
- Miller AD, Bianchi AL, Bishop BP, editors. 1997. *Neural Control of the Respiratory Muscles*. Boca Raton, FL: CRC Press.
- Miller AD, Ezure K. 1992. Behavior of inhibitory and excitatory propriobulbar respiratory neurons during fictive vomiting. *Brain Res* 578:168-176.

- Miller AD, Nonaka S. 1990. Botzinger expiratory neurons may inhibit phrenic motoneurons and medullary inspiratory neurons during vomiting. *Brain Res* 521:352-354.
- Miller AD, Nonaka S, Jakus J, Yates BJ. 1996. Modulation of vomiting by the medullary midline. *Brain Res* 737(1-2):51-58.
- Miller AD, Nonaka S, Lakos SF, Tan K. 1990. Diaphragmatic and external intercostal muscle control during vomiting: behavior of inspiratory bulbospinal neurons. *J Neurophysiol* 63:31-36.
- Miller AD, Tan LK, Suzuki I. 1987. Control of abdominal and expiratory intercostal muscle activity during vomiting: role of ventral respiratory group expiratory neurons. *J Neurophysiol* 57:1854-1866.
- Moschovakis AK, Gregoriou GG, Ugolini G, Doldan M, Graf W, Guldin W, Hadjidimitrakis K, Savaki HE. 2004. Oculomotor Areas of the Primate Frontal Lobes: A Transneuronal Transfer of Rabies Virus and [14C]-2-Deoxyglucose Functional Imaging Study. *J Neurosci* 24:5726-5740.
- Nadin-Davis SA, M. S, Abdel-Malik M, Elmgren I, Armstrong J, Wandeler AI. 2000. A panel of monoclonal antibodies targeting the rabies virus phosphoprotein identifies a highly variable epitope of value for sensitive strain discrimination. *J Clin Microbiol* 38(4):1397-1403.
- Nakazono Y, Aoki M. 1994. Excitatory connections between upper cervical inspiratory neurons and phrenic motoneurons in cats. *Journal of Applied Physiology* 77(2):679-683.
- Nattie E. 1999. CO₂, brainstem chemoreceptors and breathing. *Prog Neurol* 59(4):299-331.
- Nattie E. 2001. Central chemosensitivity, sleep, and wakefulness. *Resp Physiol* 129:257-268.
- Nattie E, Li AH, St. John WM. 1991. Lesions in retrotrapezoid nucleus decrease ventilatory output in anesthetized or decerebrate cats. *J Appl Physiol* 71:1364-1375.
- Onai T, Miura M. 1986. Projections of supraspinal structures to the phrenic motor nucleus in cats studied by a horseradish peroxidase microinjection method. *J Auton Nerv Sys* 16(1):61-77.
- Onai T, Saji M, Miura M. 1987. Projections of supraspinal structures to the phrenic motor nucleus in rats studied by a horseradish peroxidase microinjection method. *J Auton Nerv Syst* 21(2-3):233-239.
- Otake K, Sasaki H, Ezure K, Manabe M. 1988. Axonal projections from Bötzing expiratory neurons to contralateral ventral and dorsal respiratory groups in the cat. *Exp Brain Res* 72(1):167-177.
- Otake K, Sasaki H, Ezure K, Manabe M. 1989. Axonal trajectory and terminal distribution of inspiratory neurons of the dorsal respiratory group in the cat's medulla. *J Comp Neurol* 286:218-230.
- Otake K, Sasaki H, Ezure K, Manabe M. 1990. Medullary projection of non-augmenting inspiratory neurons of the ventrolateral medulla in the cat. *J Comp Neurol* 302:485-499.
- Otake K, Sasaki H, Mannen H, Ezure K. 1987. Morphology of expiratory neurons of the Bötzing complex: an HRP study in the cat. *J Comp Neurol* 258:565-579.
- Panneton WM, McCulloch PF, Sun W. 2000. Trigemino-autonomic connections in the muskrat: the neural substrate for the diving response. *Brain Res* 874:48-65.
- Poitras D, Parent A. 1978. Atlas of the Distribution of Monamine-containing Nerve Cell Bodies in the Brain Stem of the Cat. *J Comp Neurol* 179:699-718.
- Rathelot J, Strick PL. 2006. Muscle representation in the macaque motor cortex: an anatomical perspective. *Proc Natl Acad Sci U S A* 103(21):8257-8262.

- Rikard-Bell GC, Bystrzycka EK. 1980. Localization of phrenic motor nucleus in the cat and rabbit studied with horseradish peroxidase. *Brain Res* 194(2):479-483.
- Rikard-Bell GC, Bystrzycka EK, Nail BS. 1984. Brainstem projections to the phrenic nucleus: a HRP study in the cat. *Brain Res Bull* 12(5):469-477.
- Rizvi TA, Ennis M, Behbehani MM, Shipley MT. 1991. Connections between the central nucleus of the amygdala and the midbrain periaqueductal gray: topography and reciprocity. *J Comp Neurol* 303:121-131.
- Ruiz-Torner A, Olucha-Bordonau F, Valverde-Navarro AA, Martinez-Soriano F. 2001. The chemical architecture of the rat's periaqueductal gray based on acetylcholinesterase histochemistry: a quantitative and qualitative study. *J Chem Neuroanatomy* 21:295-312.
- Saper CB. 1995. Central autonomic system. In: Paxinos G, editor. *Rat Nervous System*, 2nd Edition. 525 B Street, Suite 1900, San Diego, CA 92101-4495: Academic Press Inc. p 107-135.
- Saper CB, Scammell TE, Lu J. 2005. Hypothalamic regulation of sleep and circadian rhythms. *Nature* 437(27):1257-1263.
- Sasaki H, Otake K, Mannen H, Ezure K, Manabe M. 1989. Morphology of augmenting inspiratory neurons of the ventral respiratory group in the cat. *J Comp Neurol* 282:157-168.
- Scannell JW, Blakemore C, Young MP. 1995. Analysis of Connectivity in the Cat Cerebral Cortex. *J Neurosci* 15(2):1463-1483.
- Schlenker EH, Barnes L, Hansen S, Martin D. 2001. Cardiorespiratory and metabolic responses to injection of bicuculline into the hypothalamic paraventricular nucleus (PVN) of conscious rats. *Brain Res* 895:33-40.
- Shik ML, Orlovskii GN. 1976. Neurophysiology of locomotor automatism. *Physiol Rev* 56:465-501.
- Smith JC, Ellenberger HH, Ballanyi K, Richter DW, Feldman JL. 1991. Pre-Bötzinger complex: a brainstem region that may generate respiratory rhythm in mammals. *Science* 254:726-729.
- Smith JC, Morrison DE, Ellenberger HH, Otto MR, Feldman JL. 1989. Brainstem projections to the major respiratory neuron populations in the medulla of the cat. *J Comp Neurol* 281:69-96.
- Swanson LW, Sawchenko PE. 1980. Paraventricular Nucleus: A Site for the Integration of Neuroendocrine and Autonomic Mechanisms. *Neuroendocrinology* 31(6):410-417.
- Tang Y, Rampin O, Giuliano F, Ugolini G. 1999. Spinal and brain circuits to motoneurons of the bulbospongiosus muscle: retrograde transneuronal tracing with rabies virus. *J Comp Neurol* 414(2):167-192.
- Ugolini G. 1995. Specificity of rabies virus as a transneuronal tracer of motor networks: transfer from hypoglossal motoneurons to connected second-order and higher order central nervous system cell groups. *J Comp Neurol* 356(3):457-480.
- Waldrop TG, Bauer RM, Iwamoto GA. 1988. Microinjection of GABA antagonists into the posterior hypothalamus elicits locomotor activity and a cardiorespiratory activation. *Brain Res* 444(1):84-94.
- Waldrop TG, Eldridge FL, Iwamoto GA, Mitchell JH. 1996. Central neural control of respiration and circulation during exercise. In: Rowell LB, Shepherd JT, editors. *Handbook of Physiology, Section 12, Exercise: Regulation and Integration of Multiple Systems*. New York: Oxford University Press.
- Wilkinson KA, Maurer AP, Sadacca BF, Yates BJ. 2004. Responses of feline medial medullary reticular formation neurons with projections to the C5-C6 ventral horn to vestibular stimulation. *Brain Res* 1018(2):247-256.

- Yates BJ, Billig I, Cotter LA, Mori RL, Card JP. 2002. Role of the vestibular system in regulating respiratory muscle activity during movement. *Clin Exp Pharmacol Physiol* 29(1-2):112-117.
- Yates BJ, Jakus J, Miller AD. 1993. Vestibular effects on respiratory outflow in the decerebrate cat. *Brain Res* 629(2):209-217.
- Yates BJ, Smail JA, Stocker SD, Card JP. 1999. Transneuronal tracing of neural pathways controlling activity of diaphragm motoneurons in the ferret. *Neurosci* 90(4):1501-1513.
- Yeh ER, Erokwu B, Lamanna JC, Haxhiu MA. 1997. The paraventricular nucleus of the hypothalamus influences respiratory timing and activity in the rat. *Neurosci Lett* 232(2):63-66.
- Young JK, Wu M, Manaye KF, Kc P, Allard JS, Mack SO, Haxhiu MA. 2005. Orexin stimulates breathing via medullary and spinal pathways. *J Appl Physiol* 98:1387-1395.
- Zhang J, Sampogna S, Morales FR, Chase MH. 2002. Co-localization of hypocretin-1 and hypocretin-2 in the cat hypothalamus and brainstem. *Peptides* 23:1479-1483.
- Zhang SP, Davis PJ, Bandler R, Carrive P. 1994. Brain stem integration of vocalization: role of the midbrain periaqueductal gray. *J Neurophysiol* 72(3):1337-1356.